TÉCNICO LISBOA

Regeneration of Deactivated Ni-Catalysts for CO_2 Dry Reforming

Md Abu Toyob Shahid

Thesis to obtain the Master of Science Degree in

Energy Engineering and Management

Supervisors: Prof. Francisco Manuel da Silva Lemos

Dr. Radosław Dębek

Examination Committee

Chairperson: Prof. Maria de Fátima Grilo da Costa Montemor

Supervisor: Prof. Francisco Manuel da Silva Lemos

Member of the Committee: Prof. Carlos Manuel Faria de Barros Henriques

November 2018

Special acknowledgement

This thesis is based on the work conducted within the Innoenergy Master School, in the MSc program Clean Fossil and Alternative Fuels Energy. This program is supported financially by the Innoenergy. This author also received financial support from Innoenergy, which is gratefully acknowledged.

Innoenergy is a company supported by the European Institute of Innovation and Technology (EIT) and has the mission of delivering commercial products and services, new businesses, innovators and entrepreneurs in the field of sustainable energy through the integration of higher education, research, entrepreneurs and business companies. Shareholders in Innoenergy are leading industries, research centers, universities and business schools from across Europe.

www.innoenergy.com

MSc Clean Fossil and Alternative Fuels Energy is a collaboration of:

AGH University of Science and Technology, Krakow, Poland

SUT Silesian University of Technology, Katowice, Poland

IST Institute Superior Tecnico, Lisbon, Portugal

(The MSc thesis was prepared at IST Institute Superior Tecnico, Lisbon, Portugal)

Acknowledgement

I would like to start in the name of Allah, the Most Beneficent, the Most Merciful. I would like to express my deepest gratitude and thankfulness for all the blessings.

I would like to give special thanks to my supervisor **Prof. Dr. Francisco Manuel Da Silva Lemos** and **Dr. Inz. Radosław Dębek** for their help, support in completion of this thesis.

I also would like to give thanks to prof. **Prof. Maria Amélia Lemos** for her kindness and support.

Special thank goes to **Dr. Inz. Karol Sztekler** for his continuous support from the beginning of the program.

Thanks to **Mr. Everton Santos** for his technical support in the laboratory.

I also would like to give thanks to my friends from home and abroad who support me on my journey. Special thanks to **Khadija Barhmi** for her continuous motivation.

Finally, a very special thanks goes to my parents, family, teachers, and relatives for their endless support throughout the journey.

Abstract

The objective of the study was regeneration of Ni-based catalyst that was used for DRM reaction with different mixtures of feed gas, reaction cycle time, and temperature conditions. To investigate the performance of regeneration, several types of experiments has been done. Thermogravimetry (TG) and differential scanning calorimetric (DSC) analyses were used for combustion with air (20 ml/min) for temperature from 30℃ to 800℃, combustion with air (20 ml/min) at different temperatures (700℃, 600℃, 550℃, and 500℃), pyrolysis with nitrogen (20 ml/min) for temperature from 30℃ to 800℃, and gasification of coke with carbon dioxide (80 ml/min) for temperature from 40℃ to 800℃. Simultaneous Thermal Analyzer 6000 (STA 6000, Perkin Elmer, Inc) and SDT Thermal Instrument 2960 were used for experimentation.

It has been found that lower temperature of DRM reaction promotes deposition of coke and increases with reaction cycle time. For all the cases coke regeneration started at around 500℃ and formation of plateau had been noticed over 700℃. The coke removal performance was found almost similar at 600℃ and 700℃ but higher temperature intensified the process that required less time in comparison. Deposition of volatiles containing hydrogen was confirmed by pyrolysis reaction with nitrogen. Coke gasification using carbon dioxide showed an excellent performance which can be an added advantage of DRM technology for utilization of more greenhouse gases. The DSC signal indicates deposition of several species of coke together with layered deposition of similar type species. Kinetic models were developed from the TG signal data.

Key words: TG, DSC, pyrolysis, regeneration, and gasification.

Resumo

O objetivo deste trabalho foi estudar a cinética de regeneração de catalisadores de baseados em Ni que foram utilizados para reação de DRM (reforming seco de metano) com diferentes misturas de alimentação, temperaturas e tempos de ciclo de reação. Para investigar o desempenho de regeneração, foram feitos vários tipos de ensaios. Foi utilizada a termogravimetria (TG) com calorimetria diferencial de varrimento (DSC) simultânea e foram realizados ensaios de combustão com ar (20 ml/min) com uma temperatura programada linearmente (10 ° c/min) de 30℃ a 800 ℃, combustão isotérmica com ar (20 ml/min) a diferentes temperaturas (700 ℃, 600 ℃, ℃ 550 e 500 ℃), pirólise com azoto (20 ml/min) para uma temperatura programada de 30 ℃ a 800 ℃ e gaseificação do coque com dióxido de carbono (80 ml/min) para a temperatura programada de 40 ℃ até 800℃. Em todos os ensaios foram utilizados os seguintes equipamentos: Simultaneous Thermal Analyzer 6000 (STA 6000, Perkin Elmer, Inc) e SDT Thermal Instrument 2960 (TA Instruments).

Observou-se que a reação de DRM a mais baixa temperatura promove a deposição de coque, que também aumenta com o tempo de reação. Para todos os caso a remoção de coque começa à volta de 500 ℃, atingindo um patamar por volta dos 700℃. O desempenho na remoção de coque for semelhante para as temperaturas de 600 ℃ e 700 ℃ mas a temperatura mais alta intensifica o processo de regeneração de forma que, comparativamente irá requerer menos tempo. Foi confirmado que ocorre deposição de espécies contendo hidrogénio através dos ensaios de pirólise sob azoto. A gasificação do coque utilizando dióxido de carbono mostrou um excelente desempenho e pode tornar-se uma vantagem adicional para a tecnologia de DRM na remoção de gases com efeito de estufa. O sinal de DSC parece indicar que ocorre a deposição de várias espécies de coque, ocorrendo mesmo deposição em múltiplas camadas de diferentes tipos de coque. Foram ainda desenvolvido modelos cinéticos preliminares para analisar as variações de massa observadas.

Palavras-Chave: TG, DSC, pirólise, DRM, regeneração, gasificação.

Table of contents

List of figures

List of tables

List of abbreviation

CCS: Carbon capture and storage

CCU: Carbon capture and utilization

DRM: Dry reforming of methane

DSC: Differential scanning calorimetry

DTG: Differential thermogravimetry

Ea: Activation energy

EMR: Enhanced material recovery

GHG: Greenhouse gas

K: Reaction rate constant

R: Universal gas constant

RWGS: Reverse water gas shift

T: Temperature of sample

T_f: Reference temperature

TG: Thermogravimetry

Tm: Catalyst melting temperature

Introduction

1.1 Topic overview

Among the greenhouse gases, CO_2 is the major contributor that constitutes around 76 percent of the total emissions, including those from fossil fuels, industrial processes, forestry and other land use. Next is CH_4 that accounts to almost 16 percent ("Global Greenhouse Gas Emissions Data | Greenhouse Gas (GHG) Emissions | US EPA," n.d.). The greenhouse gases trap heat in the atmosphere and this energy is stored in various component of the atmosphere. The emission of greenhouse gases has been increasing in the atmosphere from the beginning of pre-industrial period. In the last four decades, manmade CO_2 emission accounts for 50% of total accumulated CO_2 emission between 1750 and 2011 (2040 ± 310 $GtCO_2$). They were the highest from 2000 to 2010. Despite the growing number of climate change alleviation policies, the emission of CO_2 is on the rise and each year in average 1 Gt of CO_2 were added from 2000 to 2010. The effect of this can be witnessed from the mass loss of Greenland and Arctic ice sheet. The shrinking of ice sheet significantly started over the period 1992 to 2011 with a greater mass loss in the period from 2002 to 2011. As a result, sea level is rising and from 1901 to 2010 the mean sea level has risen 0.19 m globally. However, the rise depicts a growth larger than ever because since the midcentury the mean has risen more than in previous two millennia. The emission of CO_2 from the combustion of fossil fuels and industrial processes contribute with around 78% of the total greenhouse gas emission over the period 2000 to 2010. The economic and population growth are considered to be the primary driving force (IPCC, 2014).

In response to this the European Commission, comprising the EU-28 countries, has set their goals to curb the emission. The Commission already announced three stages of plans for the reduction of greenhouse gas emission, increasing the share of renewables, and increasing the energy efficiency. By 2020, the EU-28 countries want to reduce the greenhouse gas emission by 20% comparing to the emission of 1990 ("2020 climate and energy package | Climate Action," n.d.). By 2030 they fixed that target for 40% ("2030 climate and energy framework | Climate Action," n.d.) and by 2050 they want to reach the emission reduction level of 80% (from 1990 level) ("2050 low-carbon economy | Climate Action," n.d.). From the report of 2015, EU-28 countries already have surpassed 2020 goal. In 2015 the greenhouse gas emission went down to 22% in relation to the level of 1990, comprising an absolute reduction of 1265-million-ton equivalent amount of CO_2. The sector wise emission in EU-28 countries depicts that in 2015 contribution from various sectors such as fuel combustion and fugitive emission (without transport) 55%, transport sector fuel combustion including aviation 23%, agriculture 10%, industrial process 8%, and waste management 3% of the total greenhouse gas emission ("Greenhouse gas emission statistics - emission inventories - Statistics Explained," n.d.). Now EU-28 countries must push forward to meet the goal of 2030.

As power plants are the major emitters of CO_2, it is obligatory for this sector to cut down CO_2 emission. Carbon capture and storage (CCS) is a proven technology and is being considered as a strategy to curb CO_2 emission. This technology has a potential to reduce CO_2 emissions by 20% by 2050. The last step of CCS is permanent storage of CO_2, which can be implemented in a wide variety of processes such as mineral carbonation, subsurface geological storage, depleted reservoirs of oil and gas, in coal bed and various other media. Some criteria need to be considered before implementing this technology. These are: the option should be in net reduction in CO_2 emission, the identified location must have a large storage capacity, it must have the possibility of long-time isolation, cost and energy penalty should be minimal, and impact on environment should be minimized. Though CCS is a proven technology, some uncertainties need to be considered which includes post injection CO_2 behavior, the possible existence of leakage pathways, CO_2 interaction with brine rock, capillary leakage, the presence of a network of faults and fracture (Aminu, Nabavi, Rochelle, & Manovic, 2017). Another important factor to be considered is public acceptance of the technology in terms of risk perception and benefit perception (Karimi & Toikka, 2018). However, the success of CCS technology depends on public policy, government subsidy and interest that is different across the world (Thronicker, Lange, & Pless, 2016).

Due to continuous effort of the EU to go for renewable and improve efficiency as well as reducing CO_2 emissions, CO_2 capture and utilization (CCU) has become an attractive option. Carbon capture and utilization refers to the capture of CO_2 from the emission sources, followed by its distribution to different utilization options. It is estimated that CCU has the potential to process 3.7 Giga tons per year (Gt/y) which is 10% of current world emissions (Koytsoumpa, Bergins, & Kakaras, 2018). This technology offers the replacement of CO_2 extraction from natural sources. Currently CCS technology requires subsidy and economic incentives due to having high cost. Therefore, instead of considering CO_2 capture as a negative economic option, it also can be preferred as an added economic value which offers reduction in cost of CO_2 capture (Tapia, Lee, Ooi, Foo, & Tan, 2018). Utilization of CO_2 can be found in chemical and oil, food, mineralization, power, energy crops, pharmaceutical, pulp and paper, steel, and other (Koytsoumpa et al., 2018). CO_2 utilization options also can be categorized into two main classes, i.e. for chemical feedstock, and for injection in geo-structures as fluid. In the first option the CO_2 is used for the synthesis of fuel or intermediate chemicals. This option does not offer permanent remnant. Rather it reduces the dependency on the natural resources. The second option is used for enhanced material recovery (EMR). In the depleted gas and oil reservoir, shale formation for tight gas and oil, and coal bed, CO_2 is injected to enhance resource recovery. For the purpose of using CO_2 in food processing industry, meeting purification requirement is a necessary (Tapia et al., 2018).

1.2 Motivation of the work

There are three major routes involved to produce syngas from hydrocarbon through steam reforming, dry reforming and partial oxidation. Each process has its own positive and negative side based on composition of product, availability of reactants etc. Steam reforming of methane is used in petrochemical and refining industry for hydrogen production. But this route is associated with unwanted deposition of coke and excess ratio of steam to carbon is used to remove the coke. This process is extensive energy consuming process and requires more steam than the steam reforming process itself. In the contrary, dry reforming of methane is a promising potential technology for the production of synthetic gas which offers several advantages. DRM got the attraction because of having environmental and industrial benefit (Alenazey, 2014). Dry reforming of methane (DRM) reaction consumes two mains GHGs i.e. CO_2 and CH_4, which are the major contributor to global warming. This technology has become lucrative due to having large boom in shale gas development which resulted in the availability of large reserves of methane comparing to petroleum. DRM produces syngas (H_2 and CO), which is raw material for different chemical processes producing energy and chemicals (Löfberg, Guerrero-Caballero, Kane, Rubbens, & Jalowiecki-Duhamel, 2017). Synthetic gas produced with low ratio of hydrogen to carbon is suitable for downstream process like GTL (gas to liquid) fuels (Alenazey, 2014). Also, CH_4 and CO_2 produced from different processes as by product can provide an added value to the existing process. To use biogas and pyrolysis gases directly as fuels, it is needed to purify the gases i.e. remove CO_2, as CO_2 does not contribute in combustion. In fuel cell high purity of CH_4 is required for electricity generation. However, DRM technology utilizes both CO_2 and CH_4 directly and simultaneously which does not require the separation step. Thus, reduces the cost of separation. Therefore, DRM reaction provides the way for sustainable development which offers environmental protection and effectively utilizes energy resources. According to thermodynamic calculation CO_2 and CH_4 conversions were about 50% and 60% respectively at 300℃. So, activating both CO_2 and CH_4 at low temperature was feasible thermodynamically. Therefore, it is essential to search for the development of low temperature catalyst for DRM reaction (Wang, Yao, Wang, Mao, & Hu, 2018). Extensive research has been done for the development of highly active catalyst for DRM and highly resisting to formation of coke. Researches has found various highly active catalysts which are based on cobalt and nickel and promoted with noble metals. However, from the economic point of view development of non-precious catalyst like Ni are more favored (Alenazey, 2014). On the other hand, DRM technology suffers several drawbacks. High reaction temperature is required for this endothermic reaction and thermodynamically the performances are limited in most cases. Such high temperature causes sintering of active species and promotes formation of coke through methane cracking or by disproportion of CO (Boudouard reaction). And the presence of CO_2 and H_2 simultaneously causes reduction in selectivity due to unwanted water gas shift reaction. In response to this problem chemical looping has been proposed. In this process, in the first stage CH_4 reacts with catalyst and gets reduced resulted in production of syngas selectively. In the second stage the catalyst is regenerated by re-oxidizing with CO_2 (Löfberg, Kane,

Guerrero-Caballero, & Jalowiecki-Duhamel, 2017). In dry reforming of methane reaction, coke deposition is inevitable. So the deposited coke can be gasified on line by using a gasifying agent CO_2 for the better performance of catalytic reactor (Alenazey, 2014).

1.3 Objective

The purpose of the study is to analyze regeneration characteristics of a Ni-based catalyst which were used for dry reforming of methane (DRM) reaction. As Ni-based catalyst promotes deposition of coke, this phenomenon hinders catalysts performance. Therefore, DRM technology is not being scaled up for economic reasons.

Thermal analysis of the catalyst regeneration will be done by changing condition and atmospheric composition. Oxygen will be used to oxidize coke in regeneration process. In addition, investigation also will be done on the performance of the reaction at different temperatures condition.

Conducting pyrolysis analysis with nitrogen also have been planned to investigate the presence of volatiles containing hydrogen together with deposited coke.

Gasification with carbon dioxide also will be explored to check the possibility of coke gasification with carbon dioxide. If this come out to be satisfactory, this will be an added value for the DRM technology.

In addition, using the experimental data kinetic model will be built to identify apparent kinetic parameter of the reaction.

Literature review

2.1 Dry reforming of methane (DRM)

DRM is a chemical reaction that converts carbon dioxide and methane to syngas (DRM, Eq. (1)) which has high prospect to alleviate environmental challenges regarding GHG emissions. In addition, the lower ratio of H_2 to CO has the potential to produce hydrocarbon through Fischer-Tropsch process. DRM is an endothermic reaction which has optimum range of temperature between 600℃ to 1000℃ to have desirable level of conversion (Aramouni, Touma, Tarboush, Zeaiter, & Ahmad, 2018).

$$CH_4 + CO_2 \rightarrow 2H_2 + 2CO,\ \Delta H^0 = 247\ kJ/mole \quad (1)$$

According to stoichiometry, lower pressure is favorable for forward reaction. Molar ratio of CO_2 to CH_4 higher than 1, has an influence on high yield in syngas production. However, DRM is not yet mature for industrial application (Aramouni et al., 2018).

For better clarification the DRM reaction is further discussed here using chemical looping reaction for reforming of methane using carbon dioxide where the overall DRM reaction is conducted in two stages.

$$CH_4 + Sol - O \rightarrow 2H_2 + CO + Sol - R \quad (2)$$

$$CO_2 + Sol - R \rightarrow Sol - O + CO \quad (3)$$

Here “Sol” represents solid catalyst, Sol-O is the oxidized catalyst, and Sol-R is the reduced catalyst. In dry methane reforming reaction CH_4 and CO_2 are exposed to a solid catalyst in cyclic way. The solid catalyst is very vital in this reaction. It acts as oxygen carrier, producing syngas while exposure to CH_4 and getting re-oxidized while exposure to CO_2. To achieve higher selectivity and suppress unwanted reverse water gas shift (RWGS) reaction it is required to isolate syngas production environment from CO_2. To retrieve the capacity of solid catalyst and remove deposited carbon on surface, it is needed to expose the catalyst to CO_2 (Löfberg, Guerrero-Caballero, et al., 2017). Comparing with steam reforming, DRM is more endothermic reaction. In DRM, CO_2 is used as oxidizing agent whereas steam (H_2O) is used in steam reforming. In parallel to the reaction amid CO_2 and CH_4, several other reactions can also occur such as decomposition of methane (Eq. (4)), disproportion of carbon monoxide which is also known as Boudouard reaction (Eq. (5)), hydrogenation of carbon dioxide (Eq. (6)), and hydrogenation of carbon monoxide (Eq. (7)). These reactions are responsible to form carbon during DRM. The reverse water gas shift (RWGS) reaction (Eq. (8)) is dependent on specific temperature range equilibrium which exist during DRM reaction. Over 1093K, Boudouard and RWGS reaction will occur (Aramouni et al., 2018).

$$CH_4 \leftrightarrow C + 2H_2,\ \Delta H^0 = 74.9\ kJ/mole \quad (4)$$

$$2CO \leftrightarrow C + CO_2,\ \Delta H^0 = -172.4\ kJ/mole \quad (5)$$

$$CO_2 + 2H_2 \leftrightarrow C + 2H_2O,\ \Delta H^0 = -90\ kJ/mole \quad (6)$$

$$CO + H_2 \leftrightarrow C + H_2O,\ \Delta H^0 = -131.3\ kJ/mole \quad (7)$$

$$CO_2 + H_2 \rightarrow CO + H_2O,\ \Delta H^0 = -41\ kJ/mole \quad (8)$$

The Gibbs free energy calculation dictates that CH_4 decomposition mainly occurs at temperature higher than 550℃ and Boudouard reaction occurs mainly below 700℃. Therefore, the temperature ranges 550℃ to 700℃ is responsible for coke formation. The deposition of coke also influenced by carbon, hydrogen, and oxygen ratio in the raw gas. Lower ratios of O/C and H/C promotes the tendency of higher coke formation. Therefore, dry reforming is more prone to coke deposition than steam reforming (Gao, Jiang, Meng, Yan, & Aihemaiti, 2018).

2.2 Reaction mechanism

Dry reforming of methane reaction can be described in four major steps presented in Figure 1:

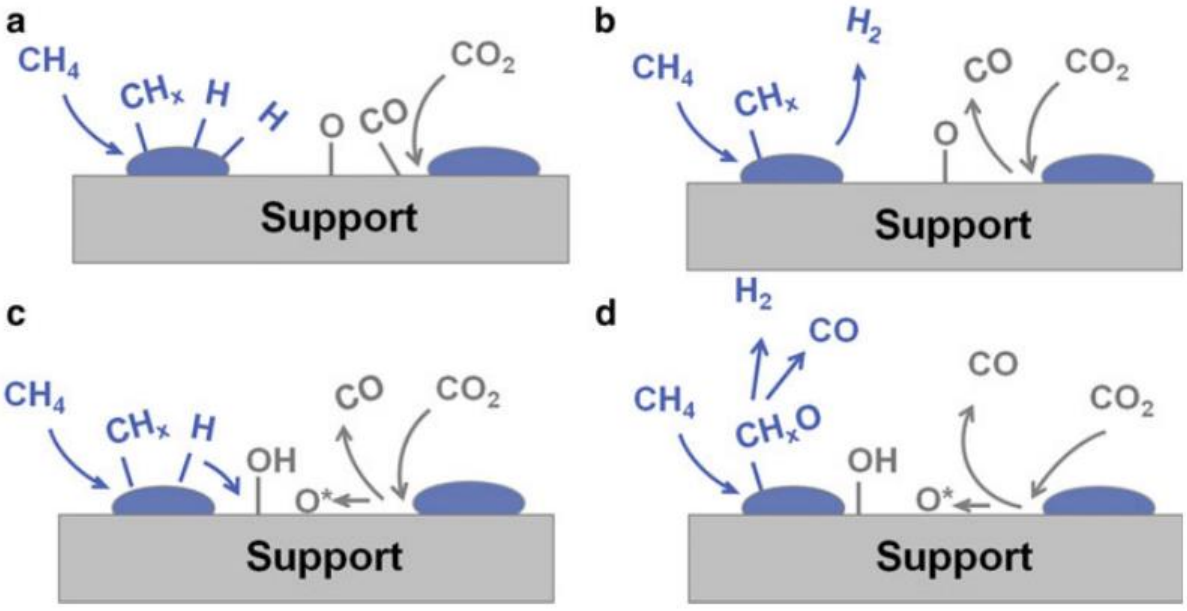

Figure 1: DRM reaction steps (Papadopoulou, Matralis, & Verykios, 2012). (a) Adsorption and separation of CO_2 and CH_4 on the interface of metal-support and metal, respectively. (b) Desorption of H_2 and CO. (c) Surface hydroxyls formation from hydrogen and spillover of oxygen. (d) Surface oxygen and hydroxyls species oxidize methyl-like surface species which are hydrogen depleted, from H_2 and CO at the final stage.

Step 1: Methane dissociative adsorption: Although surface property dictates the energy required to break C-H bond, generally methane dissociation on catalyst determines the rete of reaction. The partially dissociated hydrocarbon species search for the sites that can complete their tetra valance such CH_3- tends to be adsorbed on topmost location of metal atom where as CH_2= is adsorbed in between two metal atoms. Step sites are preferred than close packed surface for adsorption and dissociation of methane.

Step 2: CO_2 dissociative adsorption: CO_2 adsorption and dissociation are also affected by structure and defects of surface. There are three possible ways to occur such as: coordination of only carbon, coordination of carbon and oxygen (From CO_2 molecule only carbon atom and one oxygen atom are adsorbed on the surface of the catalyst leaving the other oxygen atom exposed), or coordination of only oxygen (Both of the oxygen atoms having bond with surface metal.) The last two geometric coordination are more favored for dry methane reforming. Generally, this step is fast. CO_2 has tendency to be adsorbed on metal-support interface.

Step 3: Formation of hydroxyl group: Comparing to steam reforming little work has been done on the mechanism of surface reaction for dry methane reforming. However, it is identified that water gas shift reaction (WGS) is quasi-equilibrium which means that surface reactions related to it are fast. It is predicted by most advanced model that migration of hydrogen occurs from active metal sites to support while forming hydroxyl groups below 800℃.

Step 4: Oxidation and desorption of intermediates: To form S-CO (Here S- represents surface group) or S-CH_xO, S-CH_x groups react with surface oxygen on metal particle. It is considered by some authors that S-CH_xO groups act as precursor to form CO and other authors described that carbonated formed from CO_2 reduced to CO by the carbon that is deposited on the metal. There is no strong agreement on the details of surface reaction mechanism of the catalyst (Aramouni et al., 2018).

2.3 Characteristics of catalyst: Catalyst development

Active metal: Extensive research has been done in search of active metals for catalyst which are expected to be highly active and highly resistant to coke deposition. Different noble metals have been found that fulfil the requirement of higher catalytic activity and greater reduction in coke formation. The noble metals are Pt, Pd, Rh, Ir, and Ru. Having all the required advantage, high cost limits the attractiveness of noble metals for application in industry. As a result, non-noble metals such as: Ni, Fe, and Co based catalyst due to having low cost got much attention. Among the non-noble metals, Ni is mostly studied and frequently used in industrial scale. But the obvious deposition of carbon is the major obstacle to develop Ni-based catalysts application. In response to these problem, research is continuing to identify a path, modifying with noble metals (Gao et al., 2018).

Catalyst support: Generally, a catalyst has two main components: the support material and the active metal. The support of the catalyst provides large surface area to the active metal for dispersion which allow to have large area of active sites. It is widely considered that DRM reaction goes through a bi-functional mechanism where activation of CH_4 occurs on the metal and CO_2 is activated on the acidic or basic sites of the supports. The widely studied supports are SiO_2, Al_2O_3, MgO, ZrO_2, TiO_2, La_2O_3, and CeO_2. SiO_2 is inert material due to having feeble interactions with metals and therefore less active. Because of high stability and low cost, SiO_2 is widely used as catalyst support. Al_2O_3 is also used as support in catalyst which is slight acidic. Several Al_2O_3 crystal structures have been revealed up to date. α-Al_2O_3 and ɣ-Al_2O_3 are most common in industry (Gao et al., 2018).

Catalyst promoters: Promoters are very important for increasing the performance of catalyst. It is added frequently to improve catalyst performance. Promoters can be classified in two groups: chemical (electronic) and textural (structural). Textural or structural promoters are used to enhance the structural properties of catalyst by delaying and avoiding the sintering of active element. They can also enhance catalyst stability by altering the structure or improve catalytic reaction. The function of the chemical promoters is to provide with new active added sites or to improve chemical property regarding catalyst reactivity such as redox property or basicity. More precisely the chemical promoters help to modify carbon formation for oxidizing carbonaceous species. They can also improve active metal dispersion and support gasification of deposited carbon. Alkaline and earth metals are used as promoters (Jang, Shim, Kim, Yoo, & Roh, 2018).

Basicity of catalyst: Carbon formation from the decomposition of CH_4 is usually occur on the acidic sites of support. Therefore, to determine the resistance against formation of carbon, basicity is very important property in DRM. Alkaline metals are extensively used as promoters or support. These metals reduce support acidity and to some extent act as poison, resulting in reduction of hydrocarbon cracking rate. In addition, an increase in basicity of catalyst accelerates mildly acidic CO_2 activation, that causes surface carbon oxidation (Jang et al., 2018).

Oxygen storage capacity: Oxygen storage capacity is an important factor for support that plays a role in CO_2 activation. In support, the defected oxygen sites are potential for CO_2 activation, and C-O bond cleavage, which increases the quantity of mobile oxygen on the surface of catalyst. The mobile oxygen converts C to CO by oxidizing and form intermediate species of carbonate on the basic support which is reducible. This results in elimination of carbon formation (Jang et al., 2018).

Reducibility: The novel metal and transition metallic state are generally considered to be as active phase. To reduce the metal oxide to active metal phase, an activation step is needed prior to catalytic reaction. The number of active sites available depends on the degree of reduction. In some cases, strong metal-support interaction causes poor reducibility or inactive phase formation, resulted in limited active sites (Jang et al., 2018).

Synthesis method: Synthesis method has a great influence on catalyst activity and physicochemical properties. They play a significant role in determining the metal particle size and metal-support interaction. It is important to consider required component of catalyst and material quality, when choosing the preparation method for catalyst. The most common methods are: impregnating method, co-precipitation method, and sol-gel method.

The widely used method in catalyst synthesis is impregnation. It is the outcome of capillary pressure resulting from two phase contacts of solid and liquid. The main advantage of this method is that it is reasonably easy comparing with other synthesis process. It allows a degree of control over distribution of metal on support. However, only a low amount of loading is possible through this method, and weak interactions between support and metal.

In co-precipitation synthesis method, a precipitating agent is used in solution to precipitate the active metals. Due to having the possibility to decrease the catalyst activity by precipitating agent, this process is not preferred usually.

In sol-gel method, after dissolving precursor in solution, monomers are transformed into colloidal solution through hydrolysis and condensation. This method helps to enhance thermal stability and deactivation resistance. It also has a positive influence in controlling surface area, particle size, and distribution of pore size of catalyst

In parallel to the traditional process, several other current technologies such as hydrothermal, micro-emulsion, and combustion also have been utilized (Gao et al., 2018).

2.4 Operating condition

Reaction temperature and pressure: As mentioned, DRM reaction is an endothermic process. Higher temperature stimulates the reaction to form syngas and to improve CH_4 and CO_2 conversion. Several studies have shown that CH_4 conversion increases with increase in temperature, and a similar trend also found for H_2 yield. On the other hand, formation of carbon from CH_4 decreases with the increase in temperature. Because methane cracking is an exothermic reaction and higher temperature hinder the process. Same principle also goes for hydrogenation of CO and CO_2 and Boudouard reaction. High temperature also promotes RWGS reaction, as this is also an endothermic reaction. This results in the decrease of H_2 to CO ratio, because CO is produced by consuming H_2. In case of the influence of the pressure, an increase in pressure from 1 to 30 bars, decreases CH_4 conversion and H_2 yield. Therefore, it can be outlined that for dry reforming high pressure is not appropriate (Jang et al., 2018).

Calcination and reduction temperature: Textural properties and active metal size of catalyst are influenced by calcination temperature. As a result, it is important to identify suitable calcination temperature to attain high activity of catalyst and low deposition of carbon. For Ni/Al_2O_3 catalyst, it has been found that higher activity of catalyst was obtained for calcination temperature at 300℃-450℃ than higher temperature at 600℃-750℃. Because, higher temperature of calcination causes amalgamation of NiO which resulted in formation of isolated $NiAl_2O_4$ spinel. In addition, surface area also decreases due to increase in calcination temperature (Jang et al., 2018). Reduction temperature has influence over catalyst structure, performance, and size of particles. For $ZnO_x/Ni\text{-}MnO_x/SiO_2$ catalyst, it was found that increase in reduction temperature changes crystal structure of catalyst. Increase in particle size also had been noticed with the increase in reduction temperature (Yao et al., 2017). Similar characteristics also found for catalyst Co/TiO_2 tested for DRM reaction. The catalyst (Co/TiO_2) reduced at 750℃ showed faster reforming than oxidation of surface metals while the catalyst reduced at 900℃ showed faster performance of surface metal oxidation than reforming (Takanabe, Nagaoka, Nariai, & Aika, 2005).

2.5 Catalyst deactivation and regeneration

Catalyst are subjected to deactivation with time. The rate of catalyst deactivation may be fast or slow which may remain active on the stream without losing activity for several years. However, the design engineer must be responsible for any kind of unwanted reduction of catalyst activity, which should allow either periodic replacement or regeneration of catalyst. As the remedial options are costly both from capital cost and production loss due to shut down, minimizing catalyst deactivation is most preferable. Catalyst deactivation is a complex process. It depends on several factors such as reactant and product of the reaction, catalytic material, reaction temperature and pressure, reaction mechanism. Fouling, poisoning, and sintering are some of the processes of catalyst deactivation. Fouling occurs when reactants, or intermediates, or products in the reactor are deposited on the catalyst surface, resulting in blocking of catalyst active sites. Fouling by carbonaceous species also known as "coking" is the most common type. Coke deposition can occur in several forms, including metal carbides, polymer aggregates, tar, and laminar graphite. Type and structure of coke formation depends on the type of catalyst, temperature, and partial pressure of carbonaceous components. Silica or carbon supports offer formation of little coke while acidic catalyst or supports are prone to coking. Several measures can be taken to minimize formation of coke such as shortening residence time, addition of hydrogen in the process to convert gaseous carbon into methane, minimizing upstream temperature of catalyst bed as low temperature is not suitable for gas phase carbon formation (Missen, Mims, & Saville, n.d.).

Poisoning is a result of chemisorption by compounds of the process stream which modify or block the active sites on the catalyst. The poison may bring changes in morphology of catalyst surface in several ways such

as reconstructing surface or relaxation of surface, modifying bond between support and metal catalyst. Poison toxicity is dependent on the adsorption enthalpy of the poison, and free energy of the adsorption process, which regulates the equilibrium constant of poison chemisorption. Feed stream impure compound is usually responsible for poisoning. However, the end product of the reaction may also act as poison. There are three major types of poisons such as (1) reactive molecules with heteroatoms, (2) molecules within the atoms having multiple bonds, and (3) metallic ions or compounds. The bond strength between catalyst support and poison may be strong or may be weak. The strong bond leads to loss activity which is irreversible. However, for the case of weak bond in chemisorption reservation of the loss of activity is done by eliminating feed stream impurity. Elimination of poison can be done by physical separation, or in case of poison type (1) or type (2), conversion of the poison to nontoxic compound is done through chemical treatment (for type (1) oxidation, and for type (2) hydrogenation). If the product itself is acting as poison, low conversion operation may be helpful, and/ or removal of product at intermediate stage within a multistage reactor (Missen, Mims, & Saville, n.d.).

Sintering is a result of agglomeration and growth of small crystals which forms the support or catalyst. The rearrangement of catalyst structure due to sintering causes a decrease in catalyst surface area, as a result loss of active sites. Sintering usually occurs when local temperature is approximately above one-third to one-half of catalyst melting temperature (Tm). For "dry" condition, upper limit of temperature ((1/2) Tm) is applied and when steam is present lower limit of temperature ((1/3) Tm) is applied, as steam causes reorganization of metals such as alumina, silica. Prevention of sintering can be done by doping catalyst with stabilizers so that to have high melting points to prevent small crystal agglomeration. The high melting point materials such as magnesia, alumina, and chromium are usually doped as stabilizers (Missen, Mims, & Saville, n.d.).

The performance of reactor can be affected by catalyst deactivation in several ways. A decrease in catalyst sites can result in reduction of catalytic activity and fractional conversion. However, some reactions strongly depend on metal configuration and while others solely depend on presence of metal. Therefore, the extent of affect in the performance relies on chemical reaction, catalyst deactivation process. Another way of deactivation is by blocking pores of catalyst. This phenomenon is prevalent in fouling when aggregates of materials are deposited on the surface of catalyst. This causes increase in resistance during diffusion (Missen, Mims, & Saville, n.d.).

Sometimes it is likely to restore the activity of catalyst completely or partially by chemical treatment. The process of regeneration can be slow, either because of thermodynamic limitation or resistance in diffusion due to blockage of pores in catalyst. Though at high temperature the desorption rate usually increases, prolonged exposure to high temperature of catalyst can result in sintering and loss of activity which is irreversible. If it is not possible to gasify the deposited species at lower temperature (less than sintering temperature), then the fouling or poisoning is likely to be irreversible (Missen, Mims, & Saville, n.d.).

2.6 Kinetic modeling

Kinetic models are broadly used to simulate thermal conversion method. The purpose of the simulation is to determine apparent reaction rate constant value, activation energy, and reaction model *f (α)*.

The thermal conversion rete often described as a function of temperature.

$$\frac{d\alpha}{dt} = k\,(T)\,.f\,(\alpha)\ldots\ldots(9)$$

Where *k (T)*, is reaction rate constant, and α is conversion which is expressed in terms of fraction of total mass loss. The reaction rate constant is described by Arrhenius law:

$$k\,(T) = A.\,e^{\frac{-Ea}{R}(\frac{1}{T}-\frac{1}{T_f})}\ldots(10)$$

Where *A* is pre-exponential factor, *Ea* is activation energy of reaction, *R* is universal gas constant, *T* is temperature of the sample at each instant and T_f is reference temperature (Coelho et al., 2012).

Experimental setup

3.1 Description of the samples

In this work regeneration of Ni-based catalyst used in dry reforming of methane was analyzed. The sample investigated at 550℃ DRM reaction showed a conversion of CH_4 and CO_2 around 50% and the percentage of conversion of both gases increased with the rise in temperature. The DRM reaction at 750℃ showed H_2/CO molar ratio around 1.4, whereas that for 550℃ was around 1.1. These represents that he decomposition of methane was influential in the DRM process and the preparation method of the catalyst is described in (Dębek et al., 2016). The catalytic performance was determined for a range of temperature from 550℃ to 750℃ and different environment and mixtures of feed condition. The abbreviation of the studied catalysts together with the details of conditions under which they were tested are presented in the Table 1.

Table 1: Samples references.

Name of the samples
750℃ – 24 h – Spent
650℃ – 24 h – Spent
550℃ – 24 h – Spent
750℃ – 5 h – Spent
550℃ – 5 h – Spent

The samples of catalyst “750℃-24h-Spent”, “650℃-24h-Spent”, and “550℃-24h-Spent” were investigated at 750℃, 650℃, and 550℃ respectively in isothermal condition with a feed gas mixture ratio of CH_4/CO_2/Ar = 1/1/8. The reaction cycle run for 24 hours. Other samples “750℃-5h-Spent” and “550℃-5h-Spent” were studied in 750℃, and 550℃ respectively in isothermal condition with a feed gas mixture ratio of CH_4/CO_2/Ar = 1.5/1.5/7. In this case the reaction cycle run for 5 hours.

3.2 Instruments

3.2.1 Simultaneous Thermal Analyzer (STA) 6000

To carry out experiment thermogravimetric analyzer (STA 6000, Perkin Elmer, Inc) was used. The crucible applied in the experiments was made of alumina, which has the melting point of 2000℃. The maximum temperature during the experiment was 800℃, as a result there was no risk of crucible melting.

Figure 2: Simultaneous Thermal Analyzer (STA) 6000, Perkin Elmer, Inc.

The Perklin Elmer simultaneous thermal analyzers (STA) is used to measure and analysis of heat flow together with weight change of sample. It has wide range of application in characterizing and analyzing organic, inorganic, and polymer materials. It combines thermos-gravimetric (TGA) technology with differential temperature analysis (DTA or DSC) to assure reliable results and simplified data interpretation. To maintain the accuracy with high precision latest sensor technology is used to measure weight of sample and temperature reference. It can operate with a wide range of temperature from minimum 15℃ to maximum 1000℃. Pyris software was used for monitoring and analyzing the registered data.

In thermogravimetric analysis (TGA), thermal degradation of the mass of sample is measured over time. During the experiment the sample is exposed to controlled atmosphere and heating program. TGA provides

the information of mass loss rate and the profile of thermal mass degradation. The type of reaction such as whether the reaction is exothermic or endothermic can be identified by differential scanning calorimetry as the information of heat absorbing or releasing by the sample is detected by DSC (Potential, n.d.).

3.2.2 SDT TA Instrument 2960

The SDT 2960 was used for thermal analysis of gasification reaction with carbon dioxide. Alumina crucible pan was used which has melting point of 2000℃. The maximum temperature of the experiment was 800℃. Therefore, the crucible was out of risk of melting.

Figure 3: SDT TA Instrument 2960 Simultaneous DSC-TGA Apparatus.

SDT 2960 is a combination of two measurements for thermal analysis in a single instrument. It has exceptional DSC sensitivity and TGA sensitivity together with stable baseline over a wide range of temperature. SDT 2960 is also able to compute normalized DSC data from actual weight of the sample. This instrument together with software offer the facility for characterizing material (Dsc-tga, n.d.).

3.3 Experiments

The whole experimental activity can be categorized in four major group: (a) combustion with air up to 800℃, (b) combustion with air at different temperatures such as: 700℃, 600℃, 550℃, and 500℃, (c) pyrolysis with nitrogen, and (d) gasification with carbon dioxide.

3.3.1 Combustion with air up to 800℃

First, all the samples were analyzed via raising the temperature from room temperature to 800℃. Air was used as oxidizing agent. At the beginning the equipment was purged with inert nitrogen. Then air was introduced (flow rate of 20 ml/min). In the temperature program in Figure 4, the sample was initially kept at 30℃ for 10 minutes to stabilize. After that the temperature was raised from 30℃ to 800℃ at a rate of 10℃/min. The sample was held at 800℃ for 10 minutes. This was followed by cooling step during which the temperature was reduced from 800℃ to 30℃ at a rate of 50℃/min.

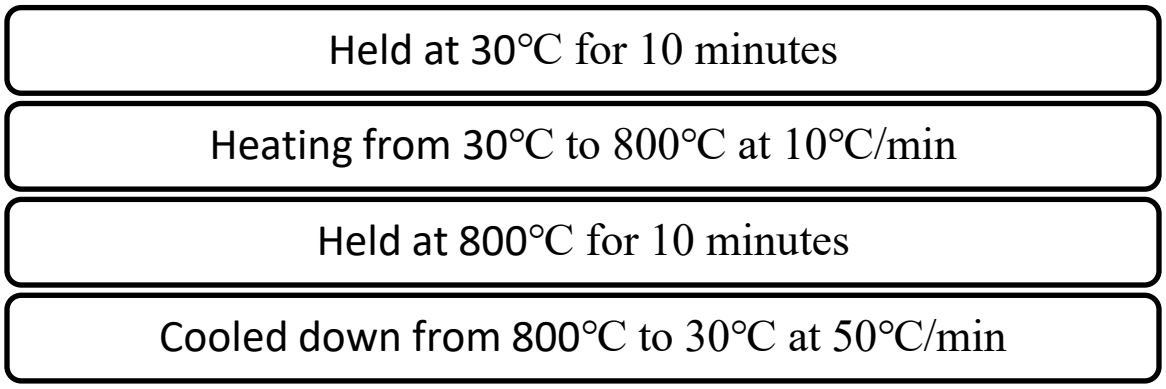

Figure 4: Temperature program of combustion experiment (30℃ to 800℃).

3.3.2 Combustion with air at different temperature

To investigate the possibility of combustion of coke at low temperature, we investigated combustion at different temperatures such as 500℃, 550℃, 600℃, and 700℃. At the beginning the equipment was purged as described before with inert nitrogen gas then it was switched to air with a flow rate of 20 ml/min. In the temperature program in Figure 5, the sample was initially kept at 30℃ for 10 minutes to stabilize. After that the temperature was raised from 30℃ to the preferred temperature at a rate of 10℃/min. The sample was held at the preferred temperature (500℃, 550℃, 600℃, and 700℃) for 60 minutes. This followed by cooling step which reduces the temperature from the preferred temperature (500℃, 550℃, 600℃, and 700℃) to 30℃ at a rate of 50℃/min.

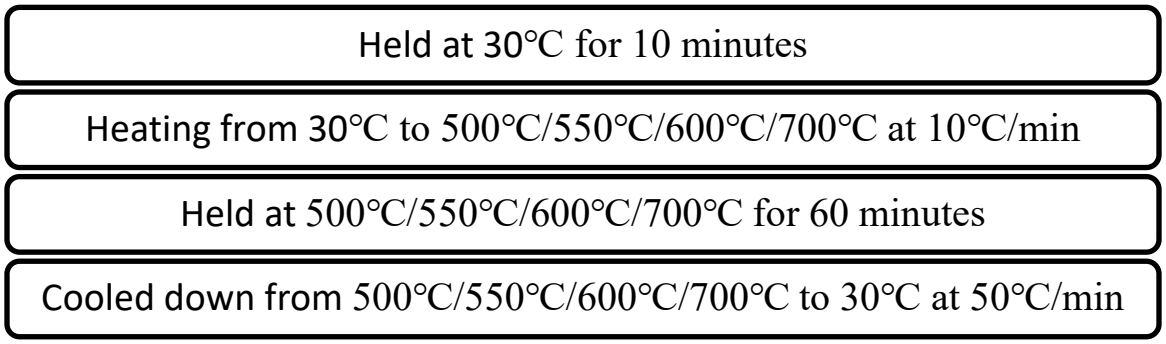

Figure 5: Temperature program of combustion experiment (30℃ to 500℃/550℃/600℃/700℃).

3.3.3 Pyrolysis with nitrogen

As dry reforming of methane involves reaction with methane and carbon dioxide, there is a possibility of deposition of hydrocarbon. This was supported by the fact that accumulation of hydrocarbon in parallel with coke as methane decomposition reaction was influential in the overall process and conversion of methane was lower than the conversion of carbon dioxide (Dębek et al., 2015). Therefore, the samples were analyzed in pyrolysis reaction with nitrogen. At the beginning the equipment was purged with inert nitrogen gas then it was switched to nitrogen with a flow rate of 20 ml/min. In the temperature program in Figure 6, the sample was initially kept at 30℃ for 10 minutes to stabilize. After that the temperature was raised from 30℃ to 800℃ at a rate of 10℃/min. The sample was held at 800℃ for 60 minutes. This followed by cooling step which reduced the temperature from 800℃ to 30℃ at a rate of 50℃/min.

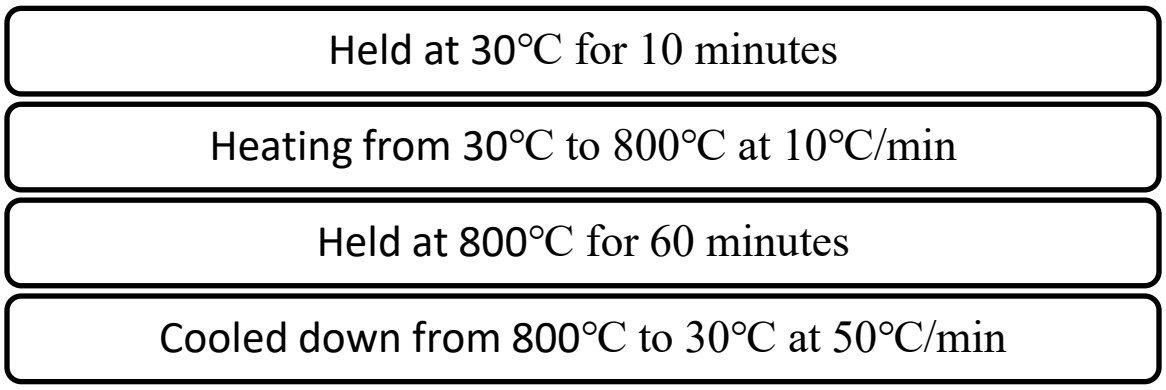

Figure 6: Temperature program of pyrolysis reaction.

3.3.4 Gasification with carbon dioxide

One of the major purposes of dry reforming of methane (DRM) reaction is to reduce greenhouse gas emission or to utilize it. If it is found to be practical the use of carbon dioxide from economic point of view, then it would be an added advantage for DRM technology. In Figure 7, at the beginning the equipment was equilibrated at 40℃. The flow rate of carbon dioxide was 80 ml/min. After that the temperature was raised from 40℃ to 800℃ at a rate of 10℃/min. The sample was held at 800℃ for 60 minutes. This followed by cooling step which reduces the temperature from 800℃ to 40℃ at a rate of 50℃/min.

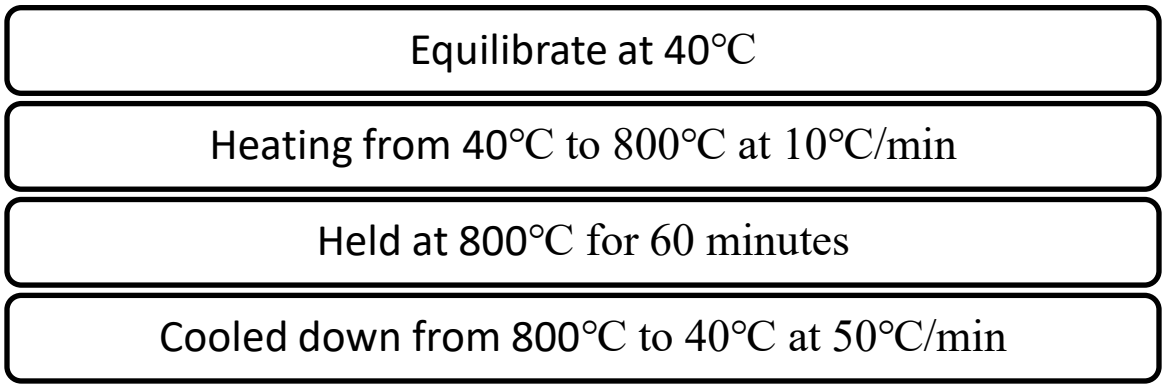

Figure 7: Temperature program of gasification with carbon dioxide.

3.4 Data processing for simulating kinetic parameters

The steps of calculating kinetic parameters are described here.

(a) After the experiment, as described above, the data file was opened with excel file.

(b) The fraction of weight was plotted on the graph versus time and temperature.

(c) The kinetic model was simulated to compute thermal degradation on mass. The concept of kinetic simulation is that we assumed some pseudo components that are converted to in thermal degradation and various other reactions such as combustion with air, pyrolysis with nitrogen, and gasifying with carbon dioxide.

(d) Regarding the pseudo components, it was also assumed that each of them follows first order reaction and they are independent from each other. Therefore, the kinetic model is applied to approximate the time-course evolution from overall conversion, and to estimate the kinetic parameters of each of the pseudo components. The expression is

$$-\frac{dWcomp\ x,n}{dt} = K(T)\ Wcomp\ x,n \quad \text{.....(11)}$$

Here, *K(T)*, reaction rate constant, provided by Arrhenius equation, *W* comp *x,n* characterizes change in each pseudo component mass fraction for a given time t_n. Euler's method is used to calculate *W* comp *x,n*.

$$W\ comp\ x,n\ = W\ comp\ x,(n-1) + \frac{dW\ comp\ x,(n-1)}{dt}\ \Delta t \quad \text{.....(12)}$$

(e) Total mass loss calculated by the model is sum of mass loss by each component.

$$W\ model,n = \sum W\ comp\ x,n \quad \text{.....(13)}$$

(f) Least square approach is used to determine the pre-exponential factor, activation energy, and mass fraction of each pseudo component. Generalized Reduced Gradient (GRG) nonlinear algorithm was used in solver tool of Microsoft Excel.

(g) In solver tool, the objective function that was set to be minimized

$$f(W)\ = \sum(W\ exp,n\ -\ Wmodel,n) \quad \text{.....(14)}$$

Where, *W exp,n* represents experimental mass loss.

Result and discussion

The experimental data analyzed and is presented here in three broad categories. The thermogravimetry analysis or mass degradation profile of combustion reaction with air up to 800℃, combustion with air at different temperatures (700℃, 600℃, 550℃, and 500℃), pyrolysis with nitrogen, and gasification of coke with carbon dioxide were presented and discussed in the thermal decomposition section. DSC signal and DTG data were presented and analyzed in the energy profile analysis section. At the end of this section kinetic modeling was developed to identify apparent kinetic parameter of the reaction.

4.1 Thermal decomposition analysis

4.1.1 TG analysis of combustion with air up to 800℃

At the beginning all the samples were analyzed through combustion reaction with air up to 800℃. In the temperature programming, the samples were set to stabilize at 30℃ for 10 minutes. Then the temperature was increased at a rate of 10℃ per minute, up to 800℃. After reaching 800℃, the samples were kept at isothermal condition for 10 minutes and then cooled to 30℃ again. The air flow to the environment set to at 20 ml per minute.

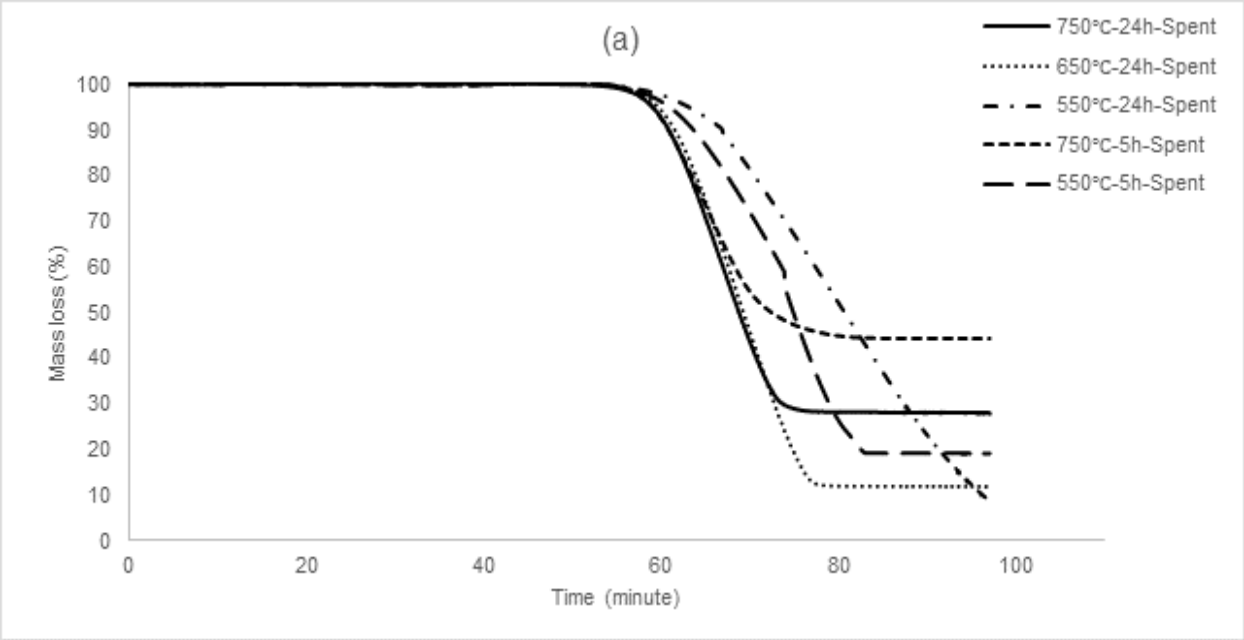

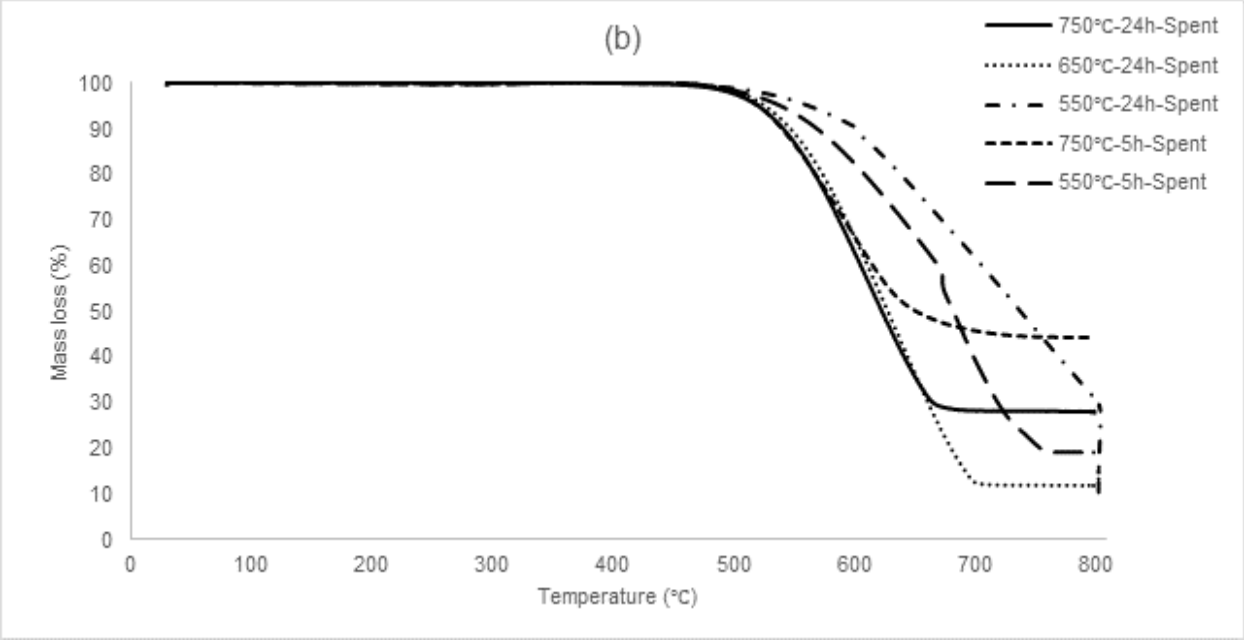

Figure 8: TG analysis of all samples for combustion with air up to 800℃ (a) with respect to time, (b) with respect to temperature.

Table 2: Mass loss (%) of all samples for combustion with air up to 800℃.

Sample	750℃-24h-spent	650℃-24h-spent	550℃-24h-spent	750℃-5h-spent	550℃-5h-spent
Mass decomposed (in %)	72	88	91	55	80

As observed in Figure 8, it can be seen that for all samples' decomposition started at around 500℃. The weight of the sample remained stable after 700℃. In general, large amount of coke deposition has been witnessed but the amount depends on the temperature of the reaction environment as well as duration of the reaction. For the case of the samples "750℃-24h-spent" and "550℃-24h-spent", the mass reduction was around 72% and 91% respectively and that for 750℃-5h-spent and 550℃-5h-spent were around 55% and 80% respectively.

So, it can be inferred that DRM reaction at lower temperature promotes higher deposition of coke. On the other hand, in terms of duration of reaction, longer cycle produced more deposition of coke for both cases.

4.1.2 TG analysis of combustion with air at different temperatures

After the combustion reaction with air up to 800℃, the possibility of oxidation of the deposited coke by air at various temperatures was investigated. Specifically, the focus was to analyze the behavior at lower temperature. Four temperatures were analyzed i.e. 700℃, 600℃, 550℃, and 500℃.

The temperature programming for combustion experiment with air, started with stabilization at 30℃ and stabilized for 10 minutes then the temperature was increased at a rate of 10℃ per minute up to the desired temperature (700℃, 600℃, 550℃, and 500℃). After reaching the desired temperature the sample was kept in isothermal condition for one hour and then cooled down to 30℃. The air flow was set to be 20 ml per minute.

Figure 9-13 provide the thermal decomposition behavior of coke at the above-mentioned temperatures for each sample.

The catalyst sample “750℃-24h-Spent” that was tested in DRM at 750℃ for 24 hours. The feed gas mixture ratio was of $CH_4/CO_2/Ar$ = 1/1/8. This used catalyst was oxidized with air at different temperatures such as 700℃, 600℃, 550℃, and 500℃. Figure 10 shows that in between 550℃ to 700℃, almost 70% of the mass was decomposed through combustion with air which can be translated as large deposition of coke. The noticeable thing is that Ni-based catalyst used at higher temperature can be regenerated or the deposited coke can be removed at lower temperature around 550℃. For 700℃ from Table 3, the thermal decomposition of sample “750℃-24h-Spent” was 72% while for 550℃ the mass decomposition was 75% which represents that higher temperature difference does not have much effect on thermal decomposition.

Sample: “750℃-24h-Spent”

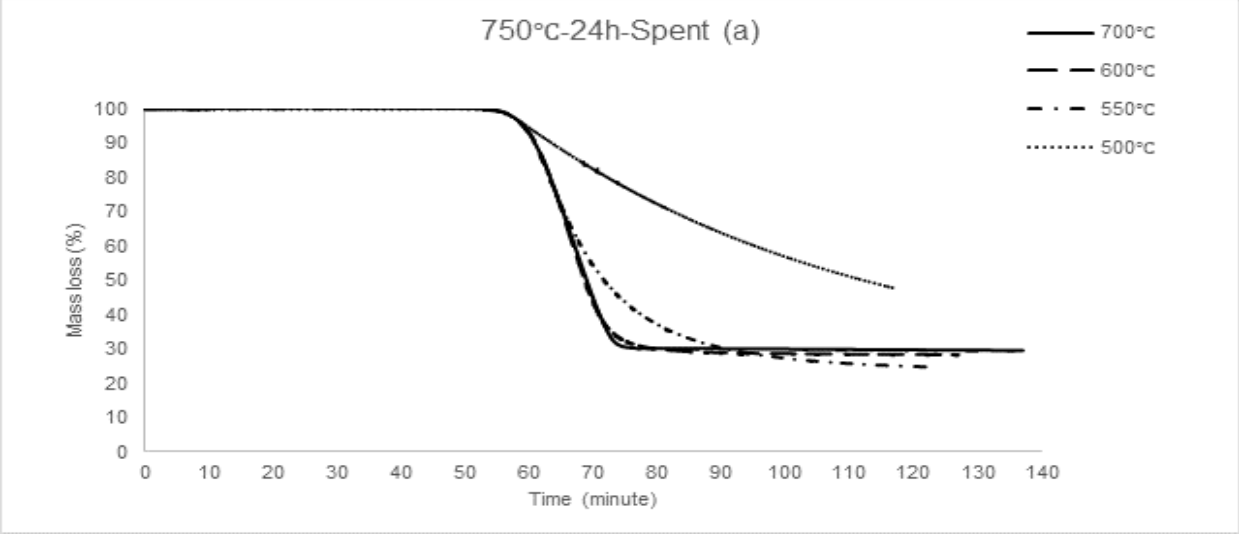

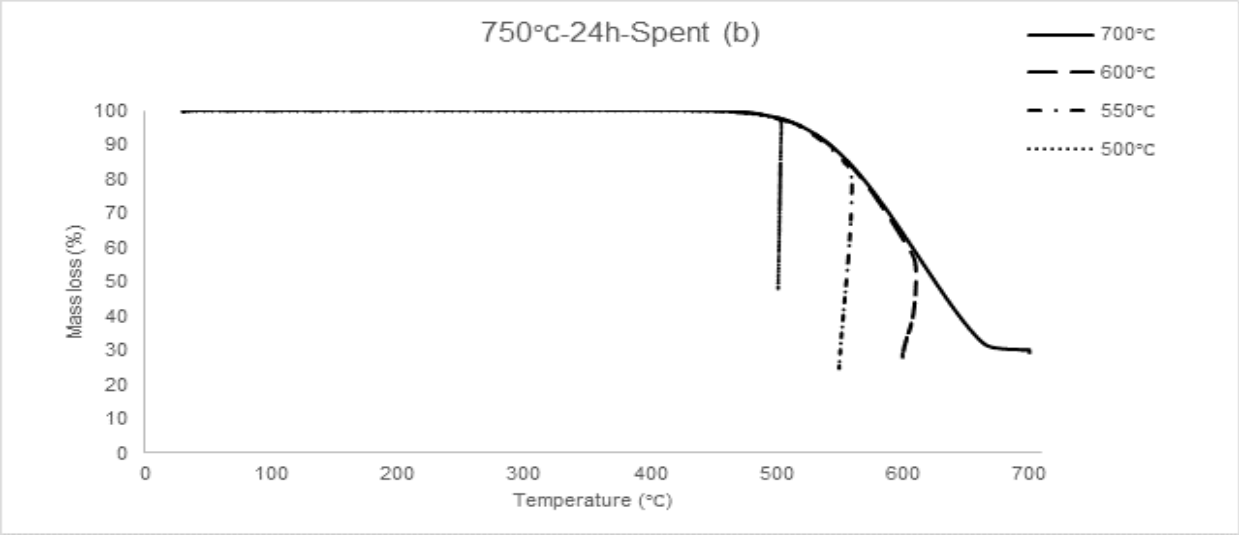

Figure 9: TG analysis of sample "750℃-24h-Spent" for combustion at different temperatures (700℃, 600℃, 550℃, and 500℃) (a) with respect to time, (b) with respect to temperature.

Table 3: Mass loss (%) of sample "750℃-24h-Spent" for combustion with air at different temperatures.

Sample	700℃	600℃	550℃	500℃
750℃-24h-Spent	70%	71%	75%	52%

For the case of the sample "650℃-24h-Spent" (Figure 10, Table 4), the catalyst was used in a reaction performed at 650℃ and the ratio of component in the feed gas mixture was CH_4/CO_2/Ar = 1/1/8. The reaction cycle was 24 hours. Figure 10 shows regeneration of the catalyst through combustion with air at different temperatures such as 700℃, 600℃, 550℃, and 500℃. As the catalyst was used in almost similar reaction environment as "750℃-24h-Spent" except temperature, the decomposition also started around 500℃. Table 4 represents that 88%, 87%, and 85% of the mass fraction was decomposed at 700℃, 600℃ and 550℃ respectively. So, coke deposition is higher for reaction temperature 650℃ than 750℃.

Sample: "650℃-24h-Spent"

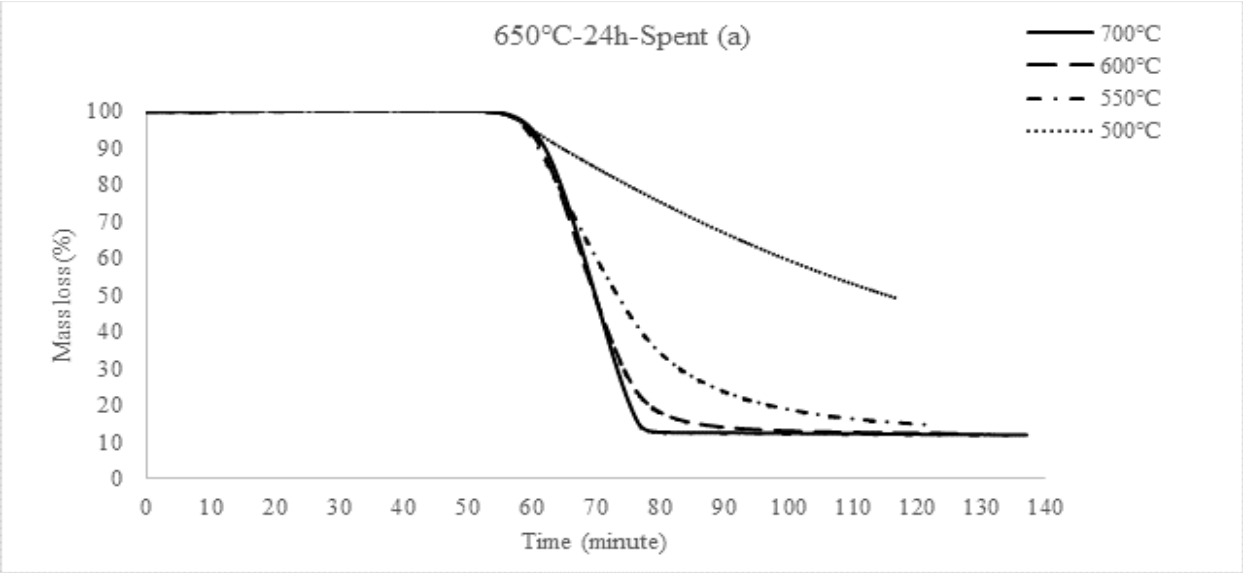

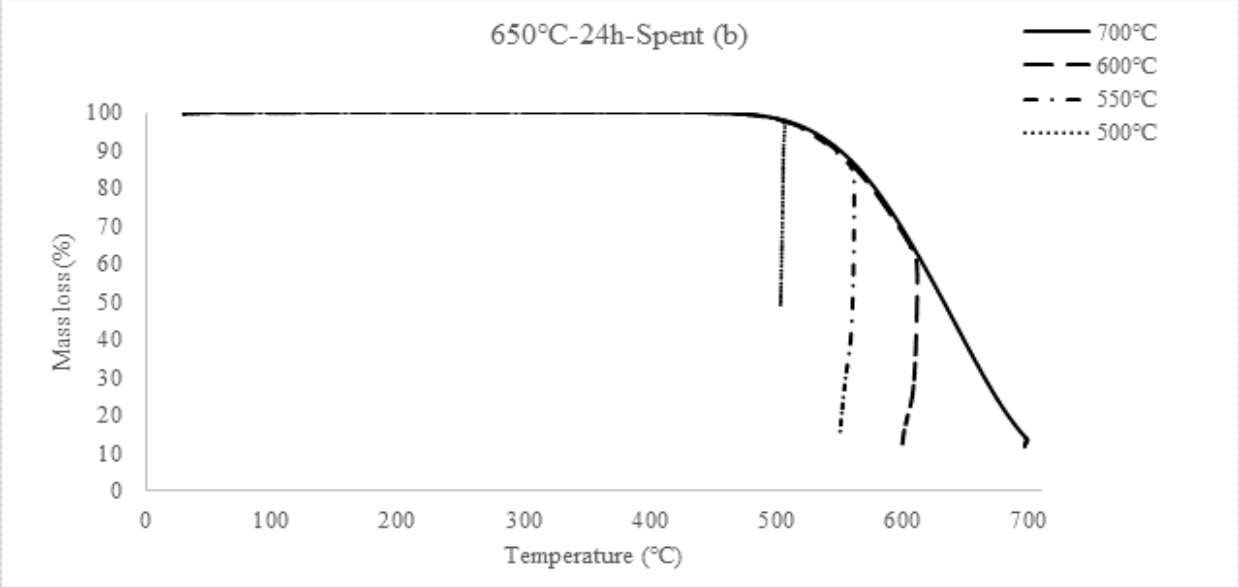

Figure 10: TG analysis of sample "650℃-24h-Spent" for combustion at different temperatures (700℃, 600℃, 550℃, and 500℃) (a) with respect to time, (b) with respect to temperature.

Table 4: Mass loss (%) of sample "650℃-24h-Spent". for combustion with air at different temperatures.

Sample	700℃	600℃	550℃	500℃
650℃-24h-Spent	88%	87%	85%	51%

The catalyst sample “550℃-24h-Spent” was tested in DRM at 550℃ and the ratio of component in the feed gas mixture was $CH_4/CO_2/Ar$ = 1/1/8. The reaction cycle was 24 hours. Figure 11 shows regeneration of the catalyst through combustion with air at different temperatures such as 700℃, 600℃, 550℃, and 500℃. The graphs represent that, in DRM reaction usually large amount of coke is deposited and in lower temperature the tendency goes higher. From Table 5, at 700℃ and 600℃ more than 95% of the mass is decomposed.

Sample: “550℃-24h-Spent”

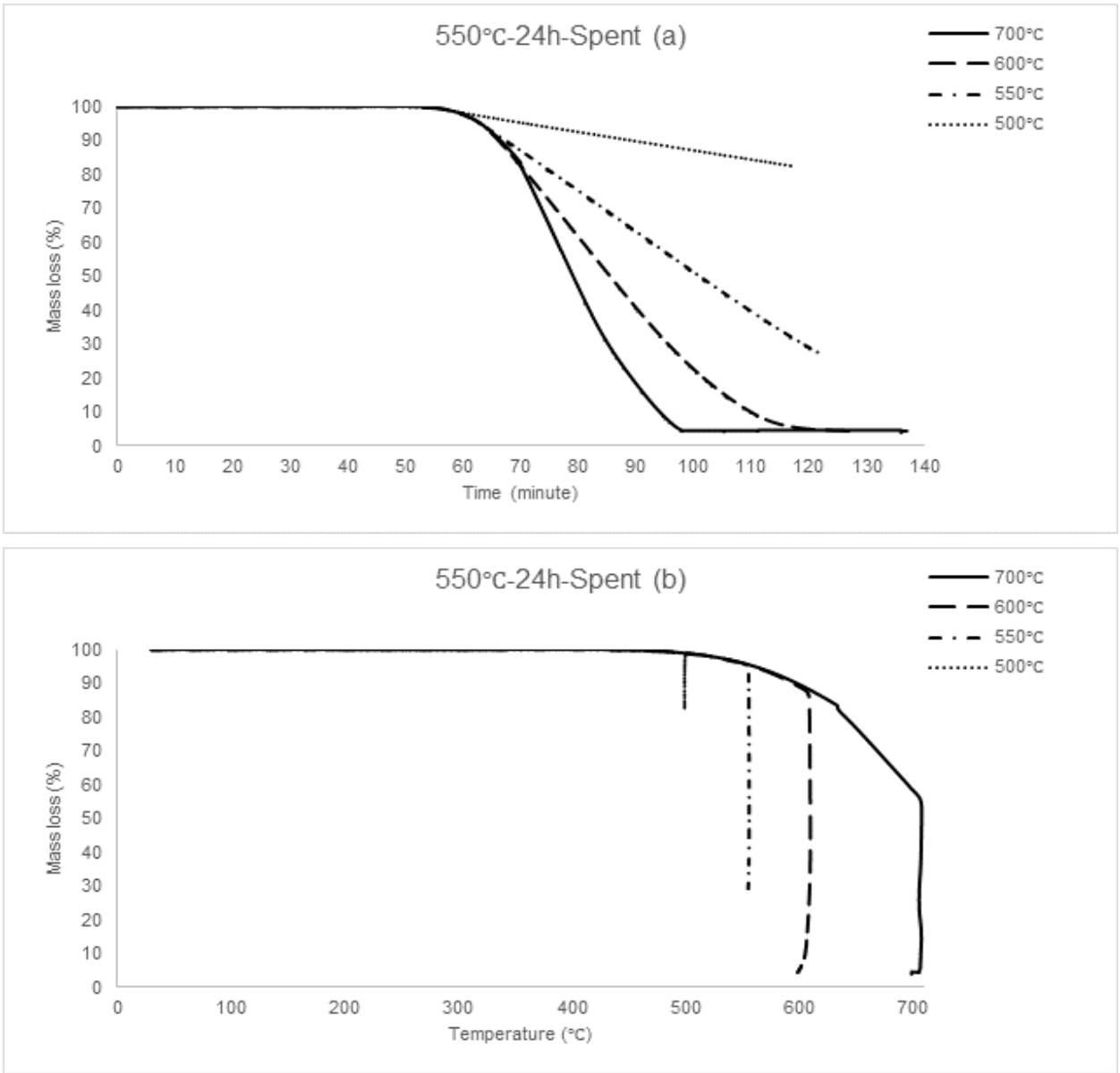

Figure 11: TG analysis of sample “550℃-24h-Spent” for combustion at different temperatures (700℃, 600℃, 550℃, and 500℃) (a) with respect to time, (b) with respect to temperature.

Table 5: Mass loss (%) of sample "550℃-24h-Spent" for combustion with air at different temperatures.

Sample	700℃	600℃	550℃	500℃
550℃-24h-Spent	95.64%	95.62%	72.9%	17.5%

Sample: "750℃-5h-Spent"

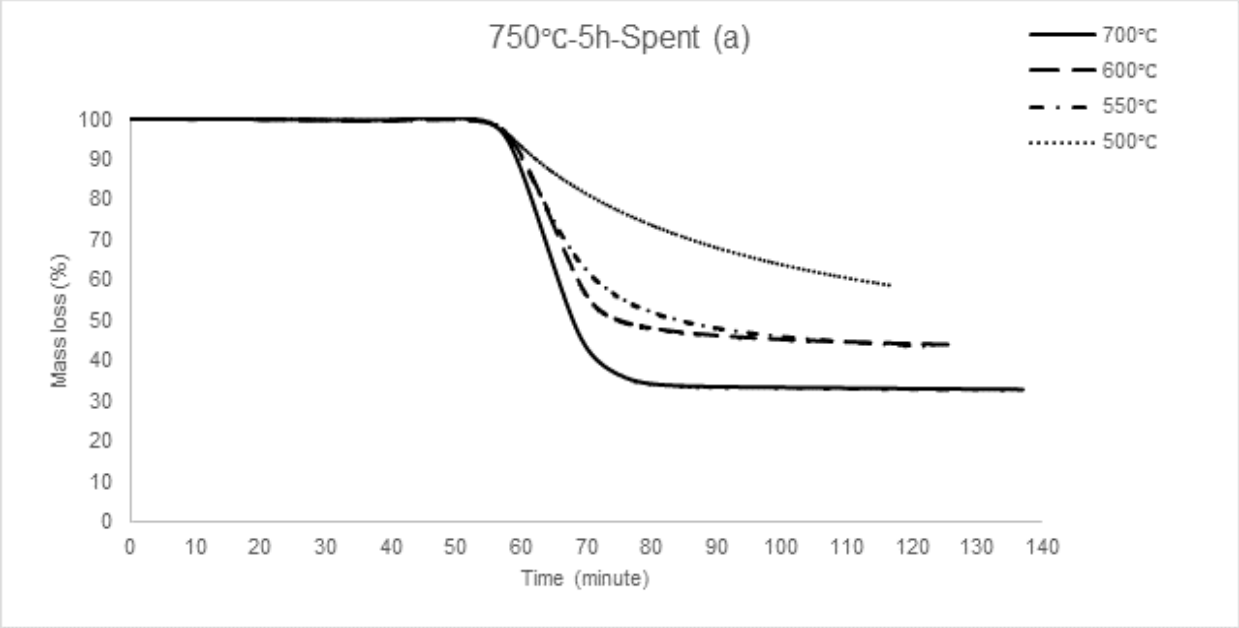

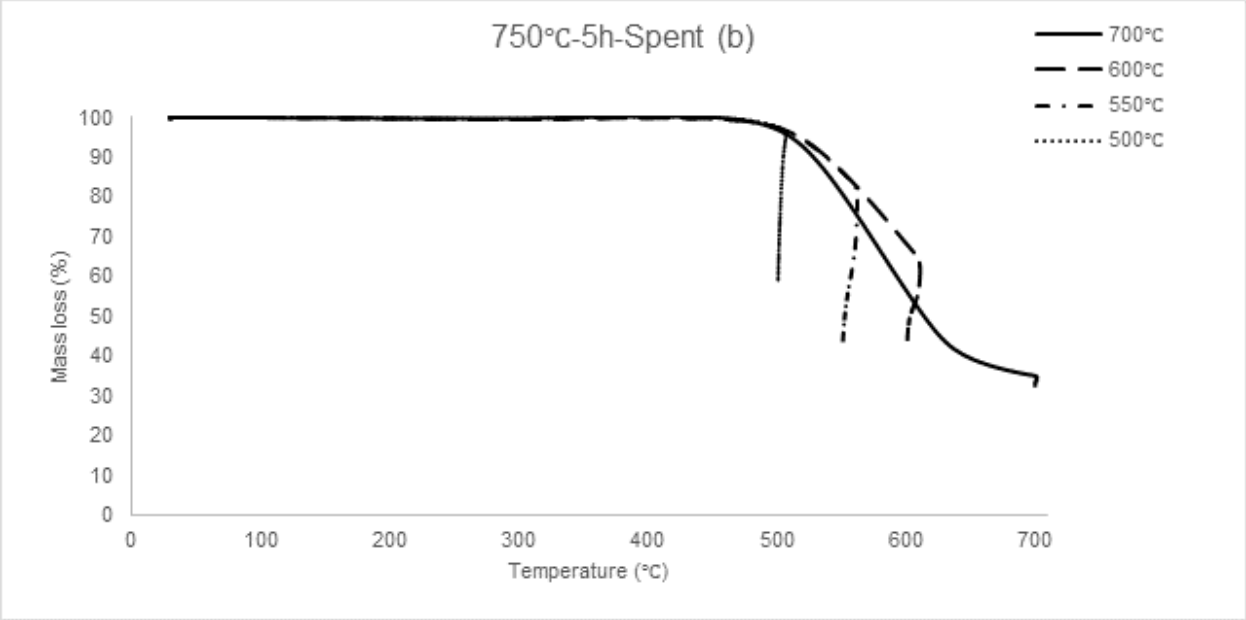

Figure 12: TG analysis of sample "750℃-5h-Spent" for combustion at different temperatures (700℃, 600℃, 550℃, and 500℃) (a) with respect to time, (b) with respect to temperature.

Table 6: Mass loss (%) of sample "750℃-5h-Spent" for combustion with air at different temperatures.

Sample	700℃	600℃	550℃	500℃
750℃-5h-Spent	67%	56%	56%	41%

In the case of the sample "750℃-5h-Spent", the catalyst was used at 750℃ for five hours and the ratio of components in the feed gas mixture was CH_4/CO_2/Ar = 1.5/1.5/7. Figure. 12 shows regeneration of the catalyst through combustion with air at different temperatures such as 700℃, 600℃, 550℃, and 500℃. The short cycle reaction (5 hours) coke deposition is comparatively lower than that of long cycle reaction (24 hour). Mass decomposition is 67%, 56%, and 56% at temperature 700℃, 600℃, and 550℃ respectively depicted in Table 6. It is noticeable that at around 550℃ and 600℃ temperature almost same amount of coke is removed.

The catalyst sample "550℃-5h-Spent" was tested in DRM at 550℃ and the ratio of component in the feed gas mixture was CH_4/CO_2/Ar = 1.5/1.5/7. The reaction cycle was for 5 hours. The sample was regenerated with air at a flow rate of 20 ml/min at different temperatures such as 700℃. 600℃, 550℃, and 500℃ and the thermogravimetry graph of the combustion reactions are shown in Figure 13. Table 7 shows the amount of mass decomposed at different temperatures which represents that at 700℃, 600℃, 550℃, and 500℃ temperature mass decompositions are 78%, 81%, 77%, and 28% respectively. In between 550℃ and 700℃, around same amount of deposited coke is oxidized but higher temperature causes the reaction faster. For the samples "550℃-5h-Spent" and "750℃-5h-Spent" the reaction environment, ratio of feed gas mixture, and reaction cycle were same except the reaction temperature. The coke deposition is higher for the samples "550℃-5h-Spent" comparing to the sample "750℃-5h-Spent". As we have witnessed for 24-hour reaction cycle, same case of coke deposition also has been witnessed for 5-hour reaction cycle that lower temperature catalytic reaction environment promotes higher deposition of coke.

Sample: "550℃-5h-Spent"

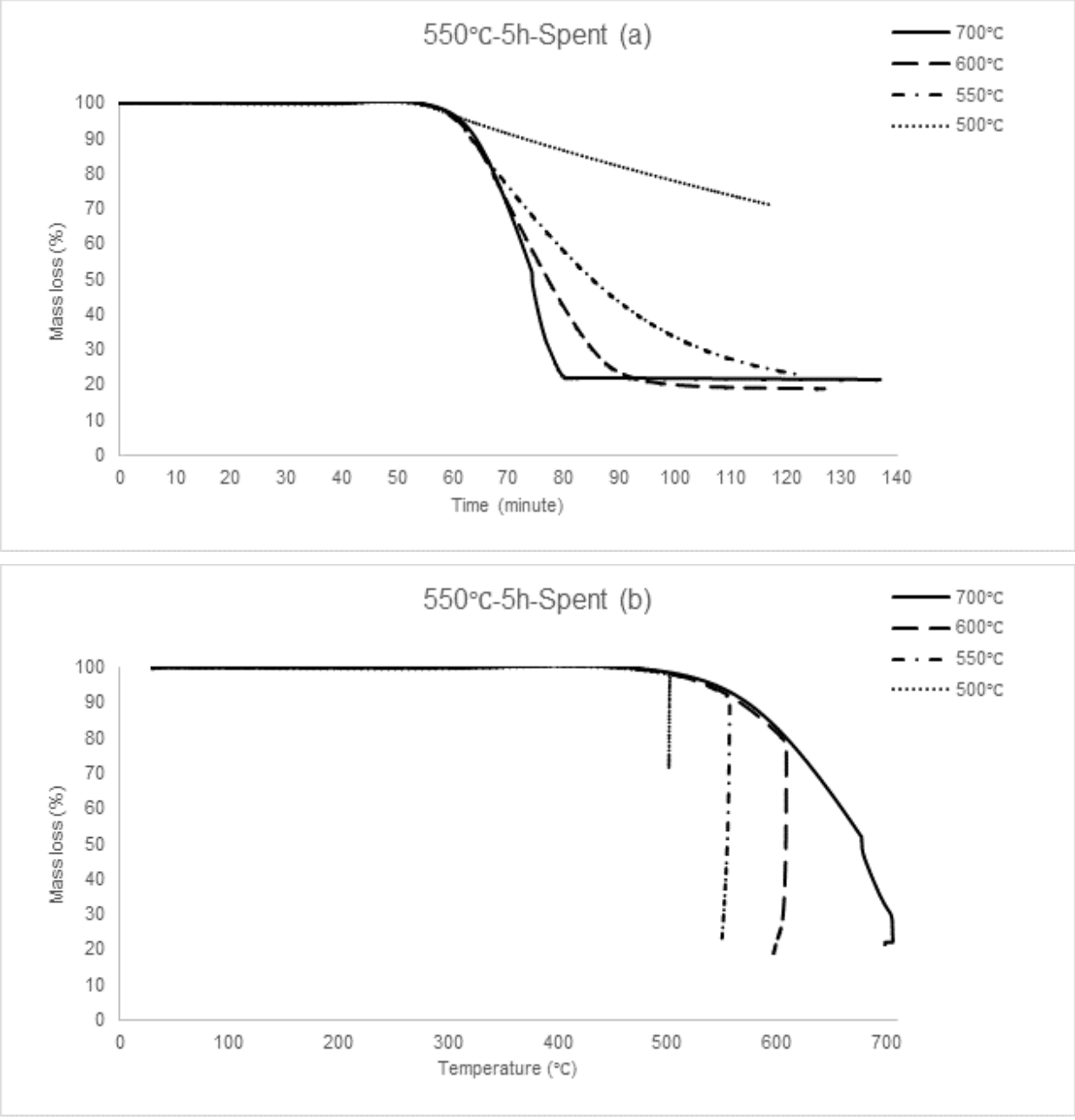

Figure 13: TG analysis of sample "550℃-5h-Spent" for combustion at different temperatures (700℃, 600℃, 550℃, and 500℃) (a) with respect to time, (b) with respect to temperature.

Table 7: Mass loss (%) of sample "550℃-5h-Spent" for combustion with air at different temperatures.

Sample	700℃	600℃	550℃	500℃
550℃-5h-Spent	78%	81%	77%	28%

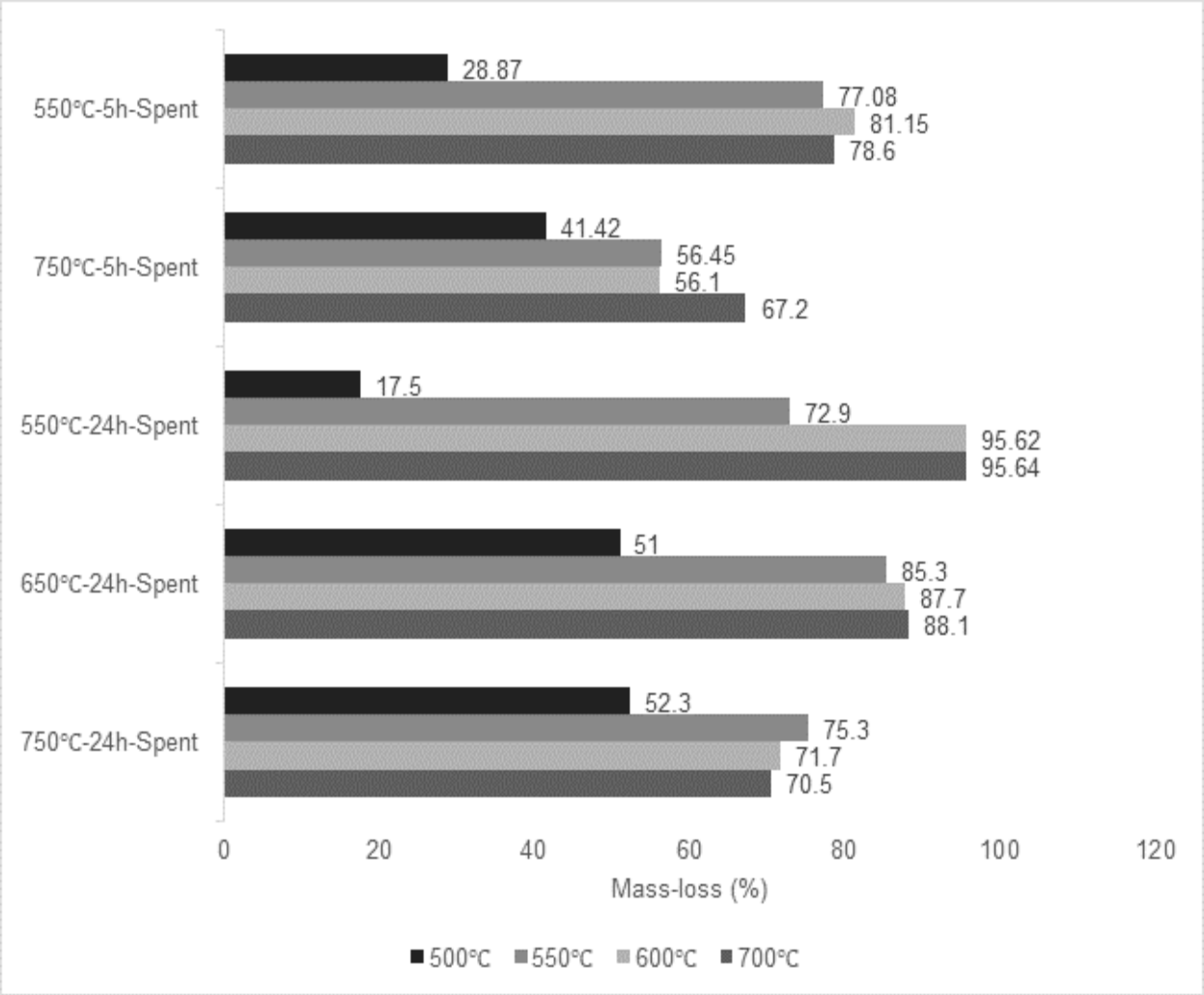

Figure 14: Comparison of mass loss (%) for combustion with air at different temperatures.

It can be analyzed from these combustion reactions with air at different temperatures that DRM causes deposition of large amount of coke on Ni-based catalyst. The amount of coke deposition depends on the reaction temperature and the duration of reaction cycle. For example: at 700℃ the mass decomposition of the sample "550℃-24h-Spent" and "550℃-5h-Spent" are 95.64% and 78.6% respectively, both occurring at the same reaction temperature but different in duration of reaction cycle. So, the longer the cycle the higher the deposition of coke. Another correlation can be inferred from the table that at higher temperature of DRM reaction, less amount of coke is deposited comparing that of low temperature DRM reaction.

4.1.3 TG analysis of pyrolysis reaction with nitrogen

The DRM reaction involves two greenhouse gas component such as carbon dioxide and methane. The theory of reaction mechanism depicts that methane molecule goes through several steps cracking process for dissociation of hydrogen from methane molecule. Therefore, there is possibility of accumulation of hydrogen containing volatiles along with coke during DRM reaction as methane decomposition reaction was influential in the overall process and the conversion of methane was lower than the conversion of carbon di oxide (Dębek et al., 2015). All the samples were investigated through pyrolysis reaction to identify the presence of volatiles bearing hydrogen together with deposited coke in an oxygen free environment. Nitrogen was used as inert gas in the reaction environment. The temperature programming for the reaction was as before, stepped up from room temperature to 800℃ and kept at isothermal condition for one hour and the flow rate of nitrogen was 20 ml per minute.

Figure 15 represents thermogravimetry graph of pyrolysis reaction of all samples in terms of time and temperature and Table 8 provides percentage of mass decomposed in the reaction. The graph depicts that the reaction or mass decomposition starts at around 500℃. The noticeable fact is that the rate of mass degradation was almost linear with function of time. As described above in the temperature programming that the sample was heated up to 800℃, thermal decomposition at higher temperatures was not analyzed. Although the sample was heated up to 800℃, the tendency of the degradation curve signifies that the sample could degrade much with higher temperature.

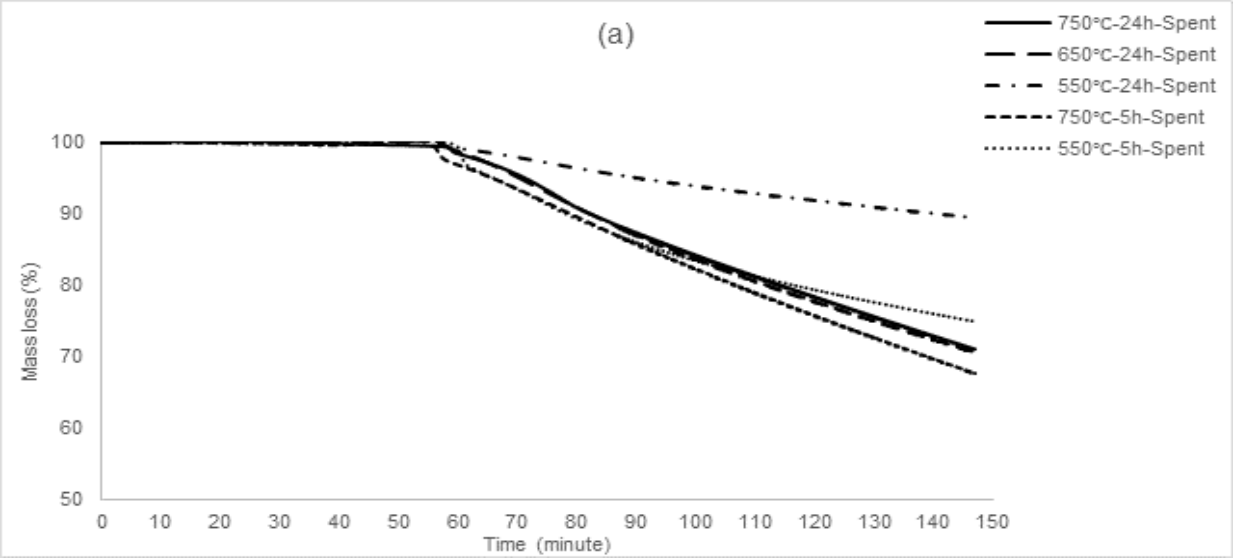

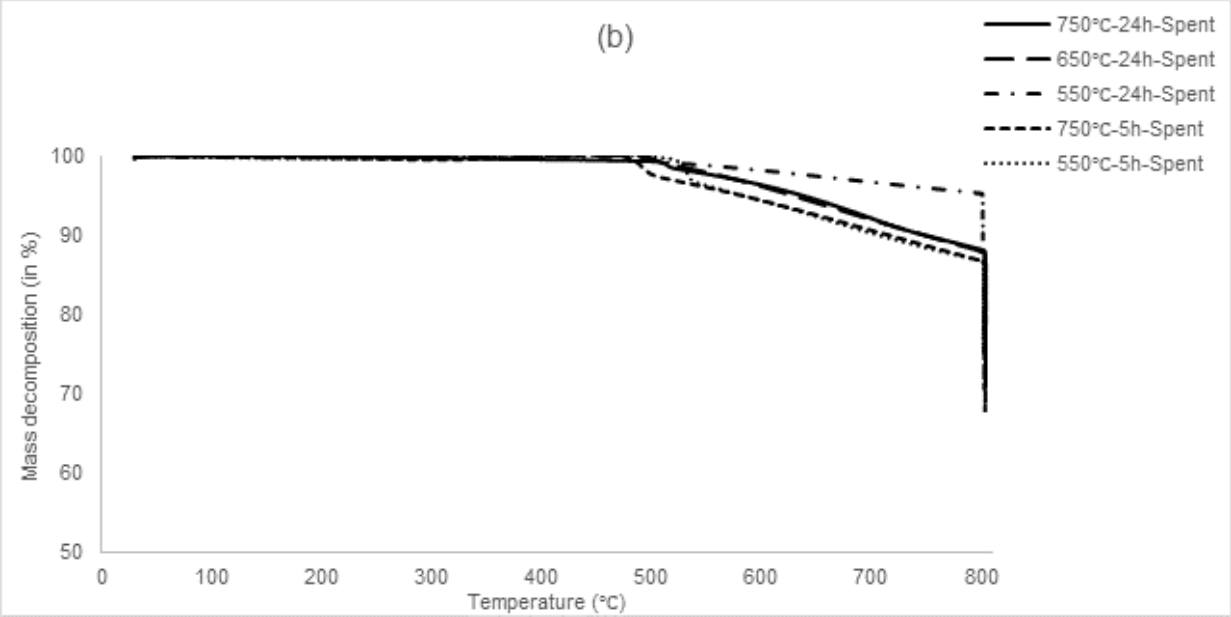

Figure 15: TG analyses of pyrolysis reaction with nitrogen of all samples: (a) with respect to time, (b) with respect to temperature.

Table 8: Mass loss (%) of pyrolysis reaction with nitrogen.

Sample	750℃-24h-Spent	650℃-24h-Spent	550℃-24h-Spent	750℃-5h-Spent	550℃-5h-Spent
Mass decomposed (in %)	28%	29%	10%	32%	25%

4.1.4 TG analysis of gasification of coke with carbon dioxide

The most attractive site of DRM reaction is that it consumes two greenhouse gases: carbon dioxide and methane. From sustainability and environmental point of view, if this technology can be developed industrially, it will have a potential impact in reduction of greenhouse gas emission. On the other hand, the main drawback of this technology is that in dry reforming of methane reaction, coke deposition is inevitable. Therefore, it will be an added advantage of the technology, if deposited coke can be gasified with carbon dioxide. It will ensure further utilization of carbon dioxide. So the deposited coke can be gasified on line by using a gasifying agent CO_2 for the better performance of catalytic reactor (Alenazey, 2014).

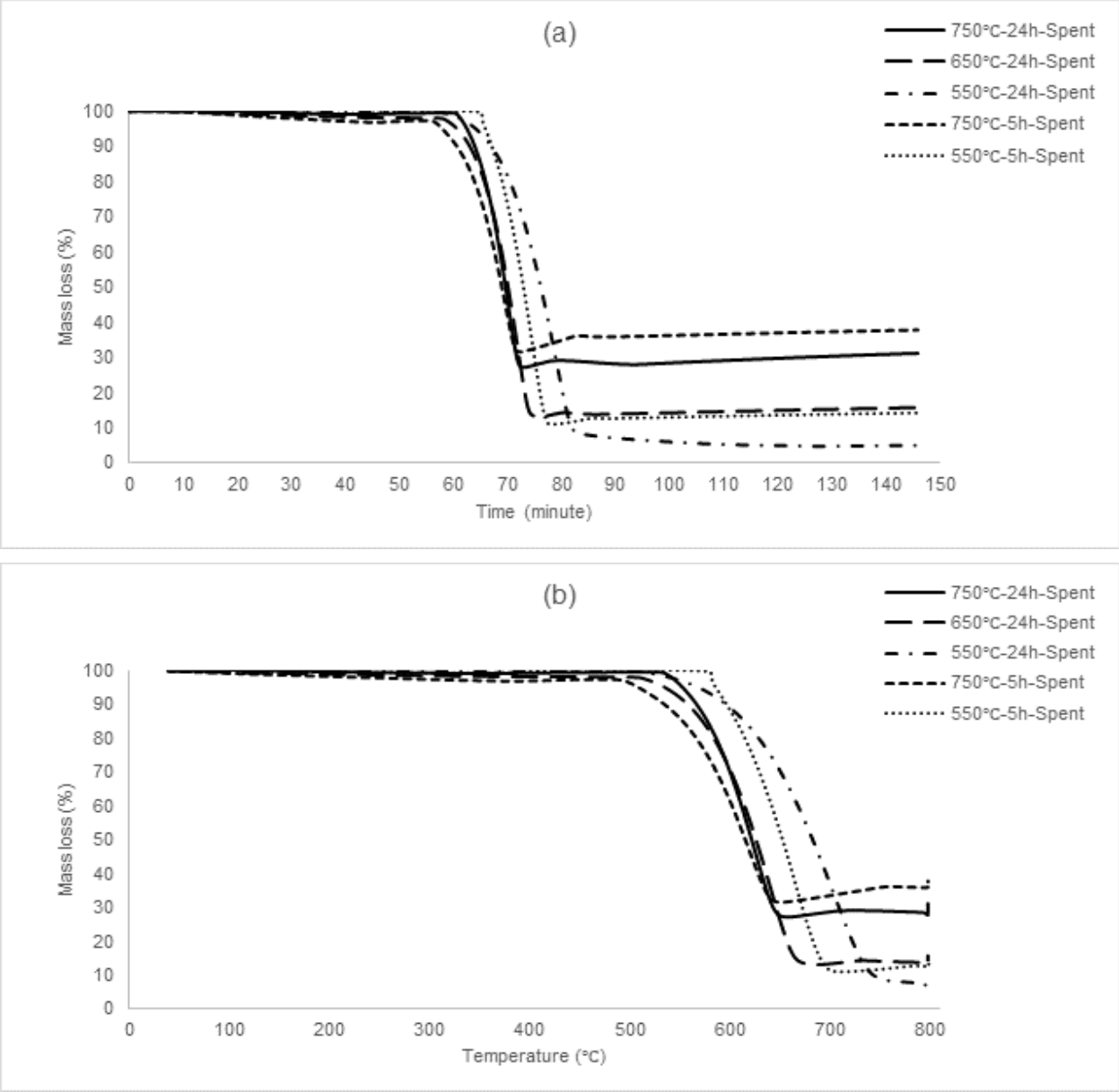

Figure 16: TG analysis of all samples for gasification of coke with carbon dioxide (a) with respect to time, (b) with respect to temperature.

Table 9: Mass loss (%) of gasification coke with carbon dioxide.

Sample	750℃-24h-spent	650℃-24h-spent	550℃-24h-spent	750℃-5h-spent	550℃-5h-spent
Mass decomposed (in %)	68%	84%	95%	62%	85%

All the samples were analyzed to gasify the deposited coke with carbon dioxide. As described in the experimental part that at the beginning all the samples were stabilized at around 40℃, then the temperature was ramped up to 800℃. The flow rate of carbon dioxide was 80 ml/min. Figure 16 represents the thermogravimetry of regeneration of catalyst through gasification reaction with carbon dioxide and Table 9 provides percentage of mass decomposed in the reaction. From Figure 16, the decomposition started at around 550℃ and the slope represents that after starting the decomposition it continued abruptly. Another significant observation is that above 700℃, there was a slight increase in mass. It might be a reaction that transform the gas phase into solid phase over 700℃. Table 9 also depicts the same as we observed before that at lower temperature coke deposition tendency is much higher. The most important finding is that the possibility of regeneration with carbon dioxide.

4.1.5 Comparison of TG analysis of combustion, gasification, and pyrolysis

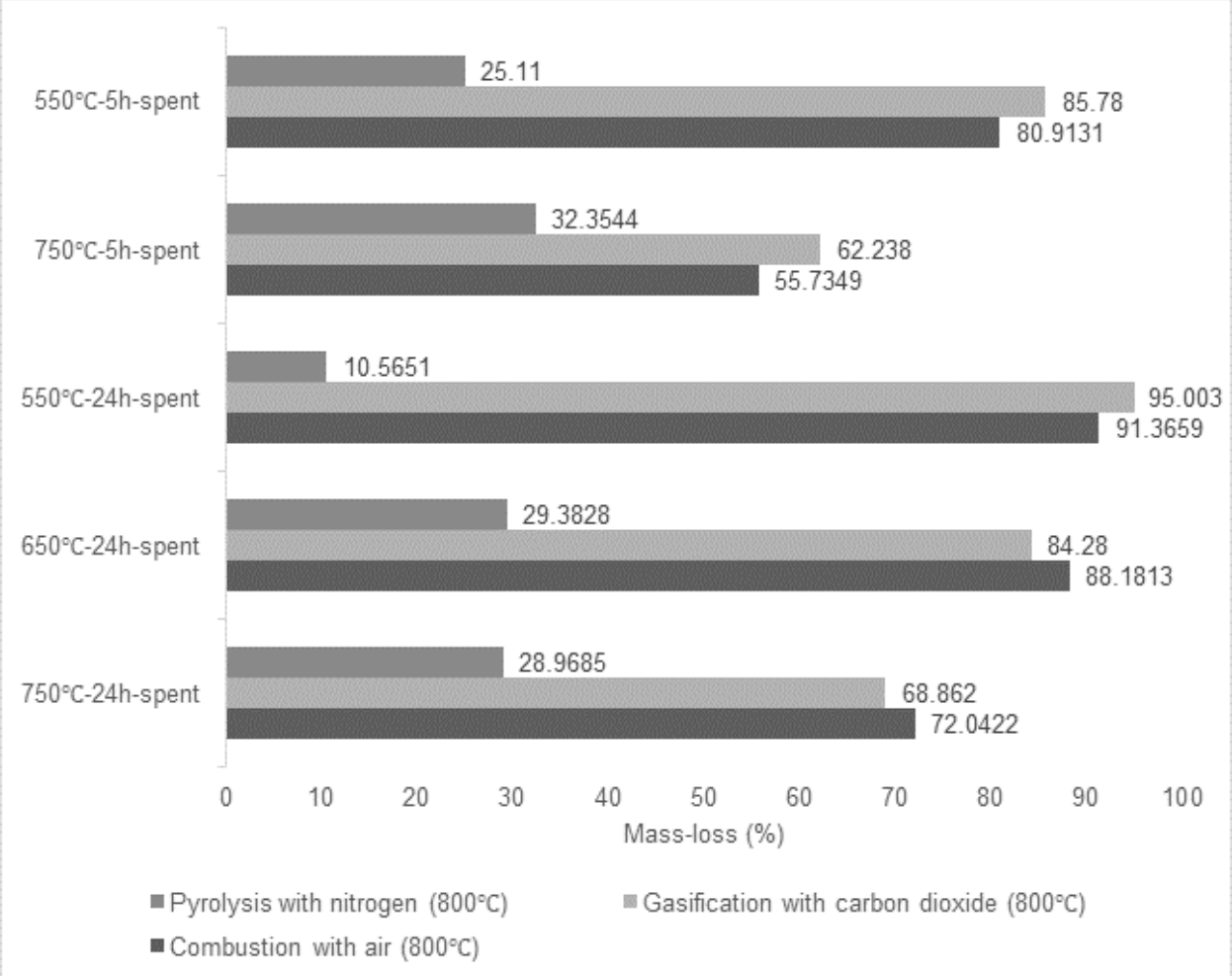

Figure 17:Comparison of mass loss among combustion, gasification and pyrolysis reactions.

Figure 17 compares the mass loss of all the samples that had been analyzed in three different reaction conditions, namely: combustion with air, gasification with carbon dioxide, and pyrolysis with nitrogen. In all the mentioned processes temperature was raised to 800℃. For gasification and pyrolysis process the samples were kept in isothermal condition for 60 minutes and in combustion reaction the isothermal retention time was 10 minutes. From the Figure 17 it can be seen that combustion with air shows better regeneration performance comparing with gasification and pyrolysis for the catalyst used in DRM reaction over 650℃ temperature and long cycle reaction. But for the catalyst used in low temperature DRM reaction environment, gasification with carbon dioxide demonstrates better performance irrespective of duration of reaction cycle. Another noticeable fact is that catalyst used in higher temperature DRM reaction with short reaction cycle illustrates better regeneration performance with gasification of carbon dioxide than combustion with air.

4.2 Energy profile analysis

The following Figures presented in this section show heat absorbed or released during the heating process together with differential thermogravimetry (DTG) data. The heat flow data is provided by differential scanning calorimetry (DSC) signal. Based on the heat flow data together with thermal degradation curve, the physical and chemical activity can be anticipated but not in a certain manner.

4.2.1 DSC-DTG analysis of combustion with air up to 800℃

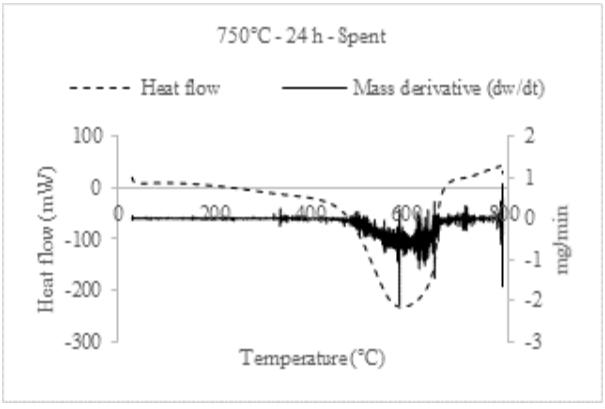

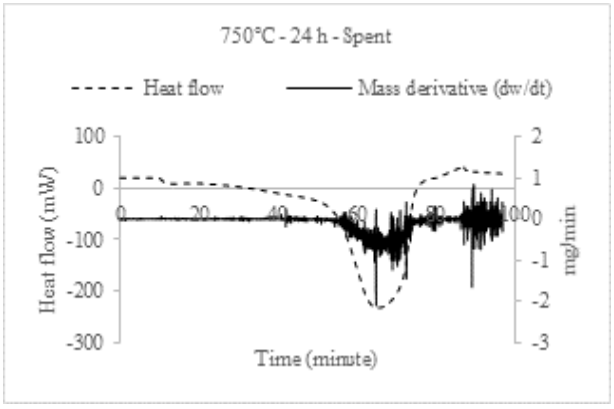

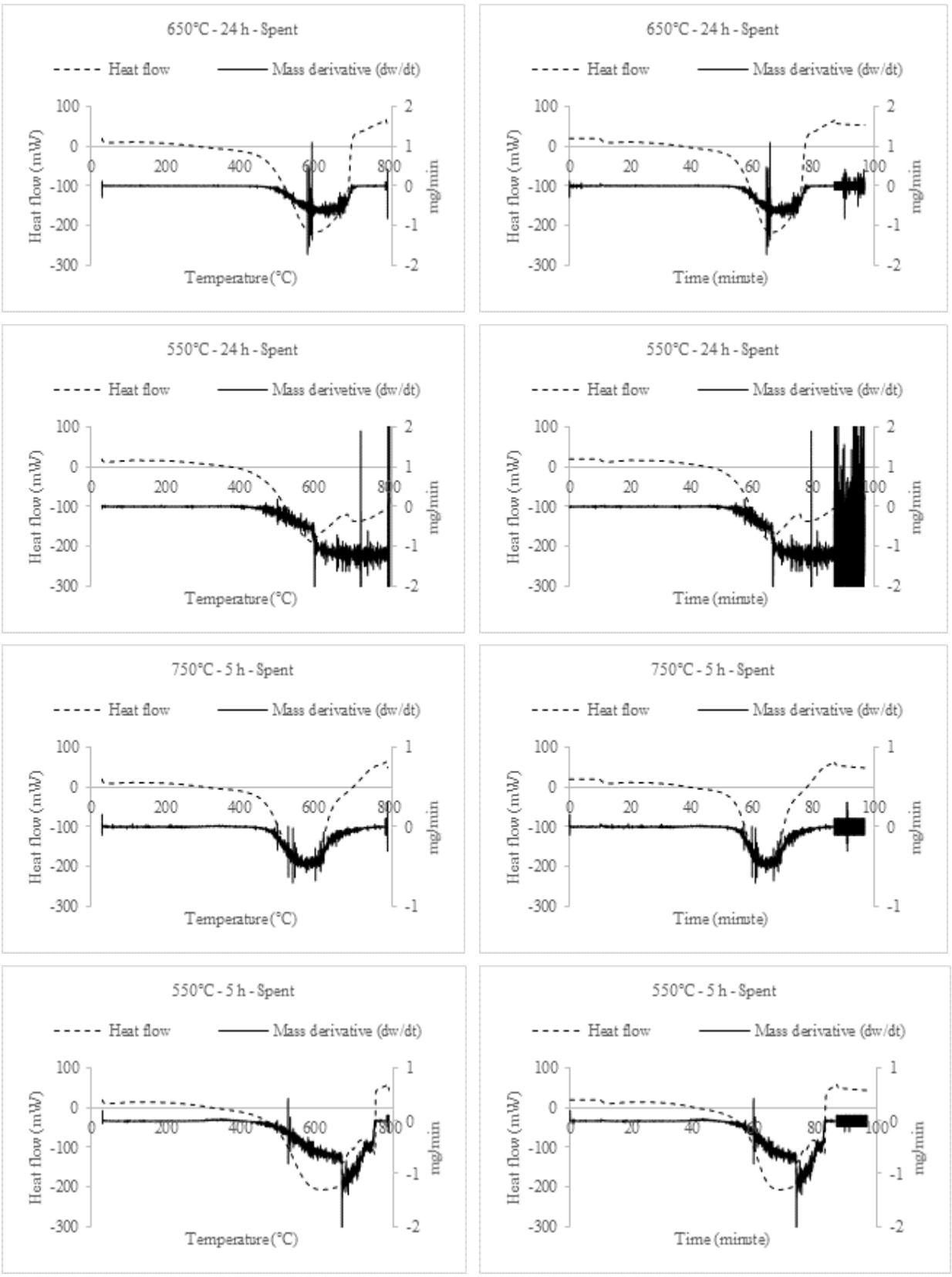

Figure 18: Heat flow and mass derivative of all samples (30℃ to 800℃).

Figure 18 shows heat flow and differential thermogravimetry data in terms of temperature and time for combustion reaction of all samples up to 800℃ where the heating rate was 10℃ per minute and samples were kept at isothermal condition for 10 minutes at 800℃. It is noticeable in the figure that at around 400℃ the sample showed an exothermic trend. At around 500℃, partial oxidation of coke was also noticed which continued with a higher reaction rate and with the rise in temperature. The peak of the reaction is reached at around 600℃. From the thermogravimetry analysis curve it may be also noticed that the fractional mass degradation started at around 500℃. The degradation continued to increase almost linearly.

It can be generalized that at around 400℃, decomposition of large molecule started but it did not vaporize. That is why no change can be seen in the thermogravimetry curve at around 400℃ temperatures. With the rise in temperature the fragmented small molecules started to vaporize at around 500℃ and it continued with the increase in temperature and became faster. After the exothermic reaction the baseline went little up comparing to pre-exothermic reaction baseline. This indicates that the post-combustion components had much higher heat capacity.

From heat flow curve it also can be interpreted that coke deposition occurred in a layered manner. Therefore, overlap in the reaction peak is noticeable. Another distinguishable fact is that the catalysts used in higher temperature environment around 650℃ or above, less variety of coke species are deposited. In terms of characteristics, these components do not differ a lot. For low temperature reaction environment (550℃) a much larger variety of coke species were deposited.

4.2.2 DSC-DTG analysis of combustion with air at different temperatures

In this section DSC and DTG curve will be analyzed for all samples which were oxidized with air at different temperatures (700℃, 600℃, 550℃, and 500℃).

Figure 19 shows heat flow and differential thermogravimetry data in terms of temperature and time of the sample “750℃-24h-Spent” at different temperatures (700℃, 600℃, 550℃, and 500℃). The temperature program is proved in Figure 5. For all cases, the exothermic reaction started to begin at around 400℃ where decomposition started. At this stage heat was mostly used to break bonds, but evaporation of fragmented components did not start. At around 500℃ reactions starts and intensifies with the rise in temperature. The reaction that was conducted up to 700℃, showed an overlap and completion of exothermic reaction. The other experiment that was conducted up to 600℃, displayed an exothermic peak had been reached but missing another limb of the peak. It might be the reason that further rise in temperature was required for the completion of exothermic reaction. In case of the reaction conducted on 550℃ and 500℃, the exothermic reaction started partially but could not go further due to lack of required higher temperature.

Sample: "750℃-24h-Spent"

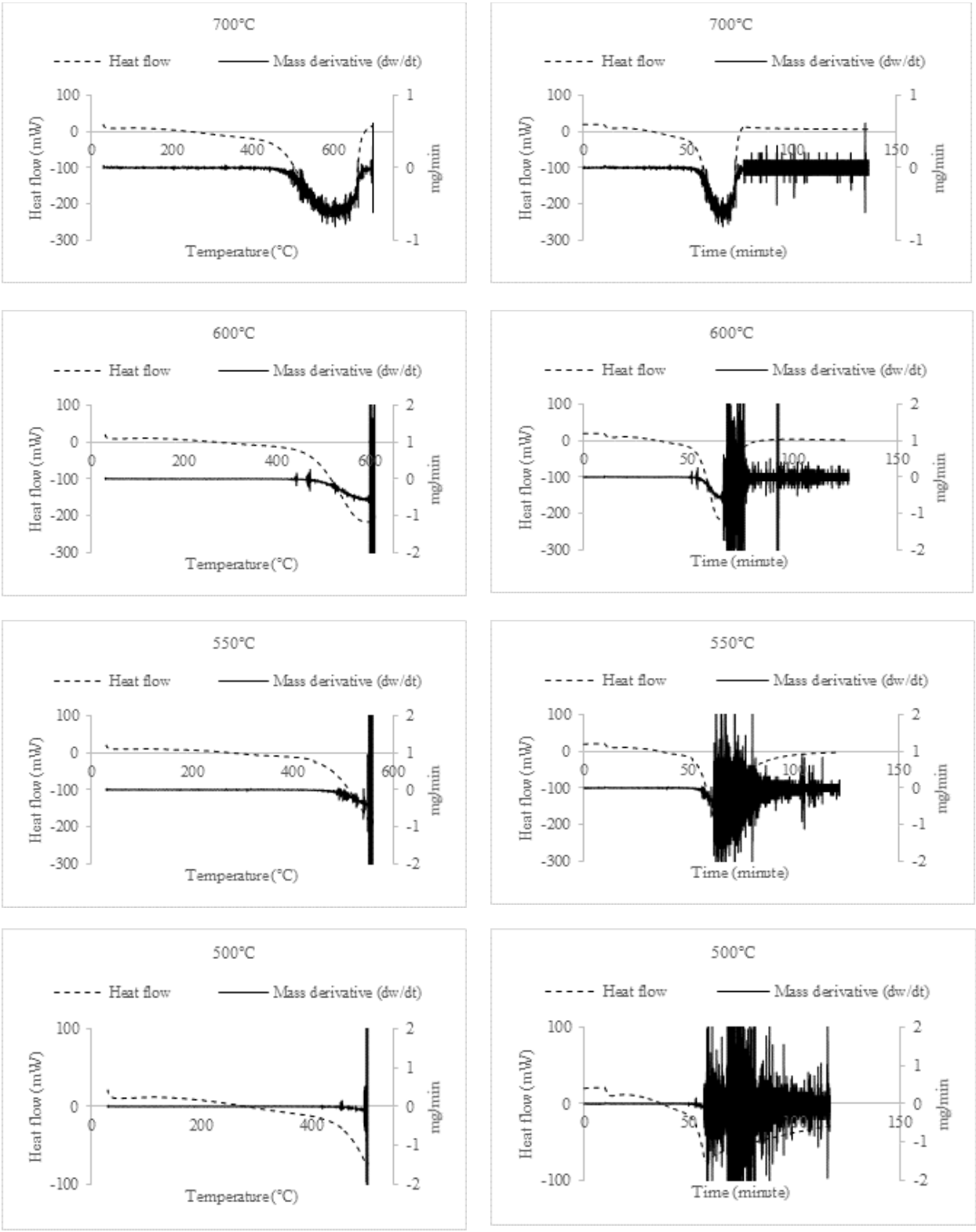

Figure 19: Heat flow and mass derivative of sample "750℃-24h-Spent" for combustion at different temperatures (700℃, 600℃, 550℃, and 500℃).

Sample: "650℃-24h-Spent"

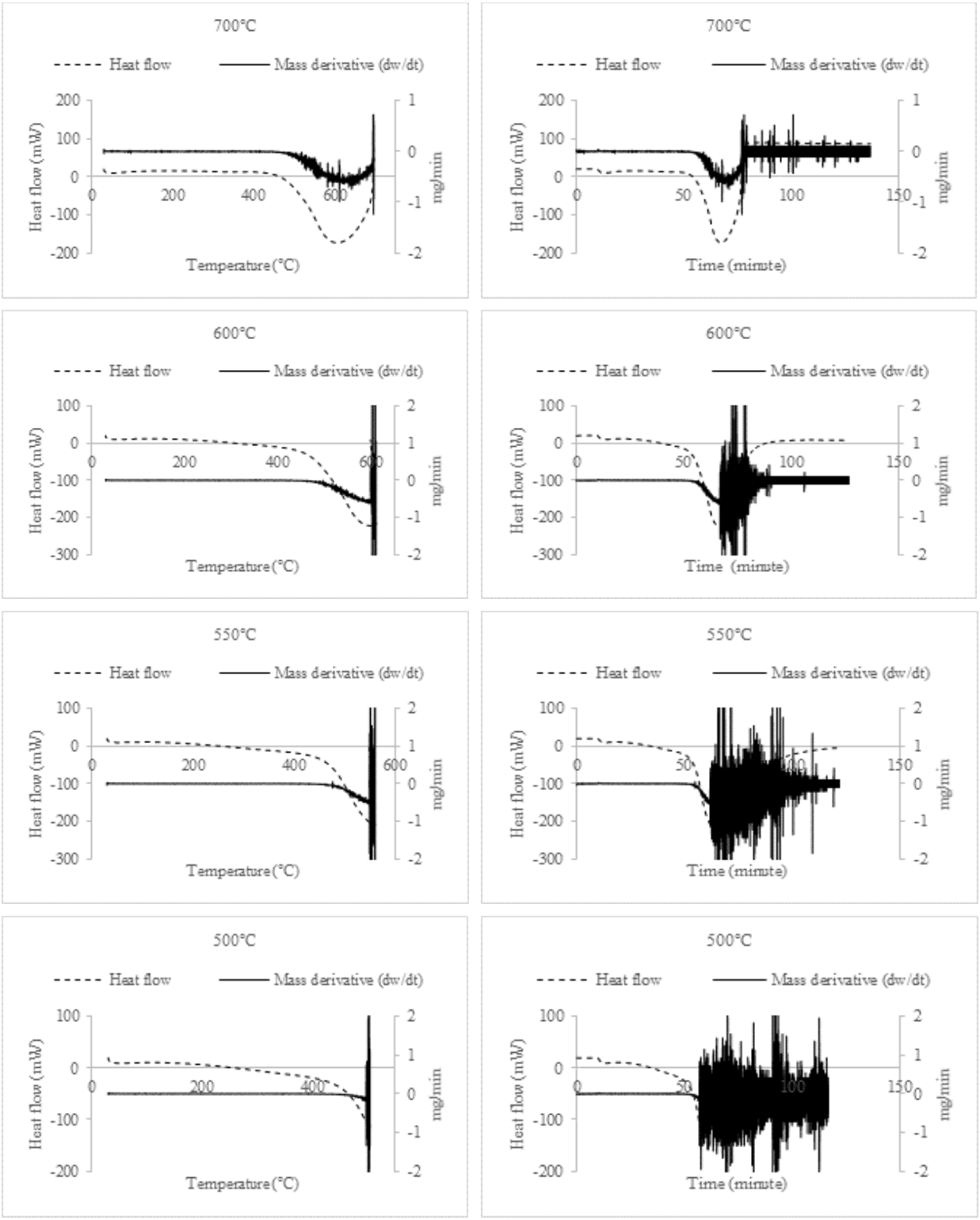

Figure 20: Heat flow and mass derivative of sample "650℃-24h-Spent" for combustion at different temperatures (700℃, 600℃, 550℃, and 500℃).

Figure 20 illustrates data recorded for sample “650℃-24h-Spent” where heat flow and derivative of mass degradation is depicted in terms of temperature and time for combustion reaction with air at four different temperatures (700℃, 600℃, 550℃, and 500℃). The heat flow and differential thermogravimetry curves for the reactions demonstrates almost similar behavior as it was analyzed for the sample “750℃-24h-Spent”. For all the cases, the breakage of bond starts at around 400℃ and combustion starts at around 500℃. The experiment that is conducted up to 700℃ shows completion of exothermic reaction with overlap. This explains that catalyst used in a reaction environment of 650℃ causes deposition of coke in layered strata.

Sample: “550℃-24h-Spent”

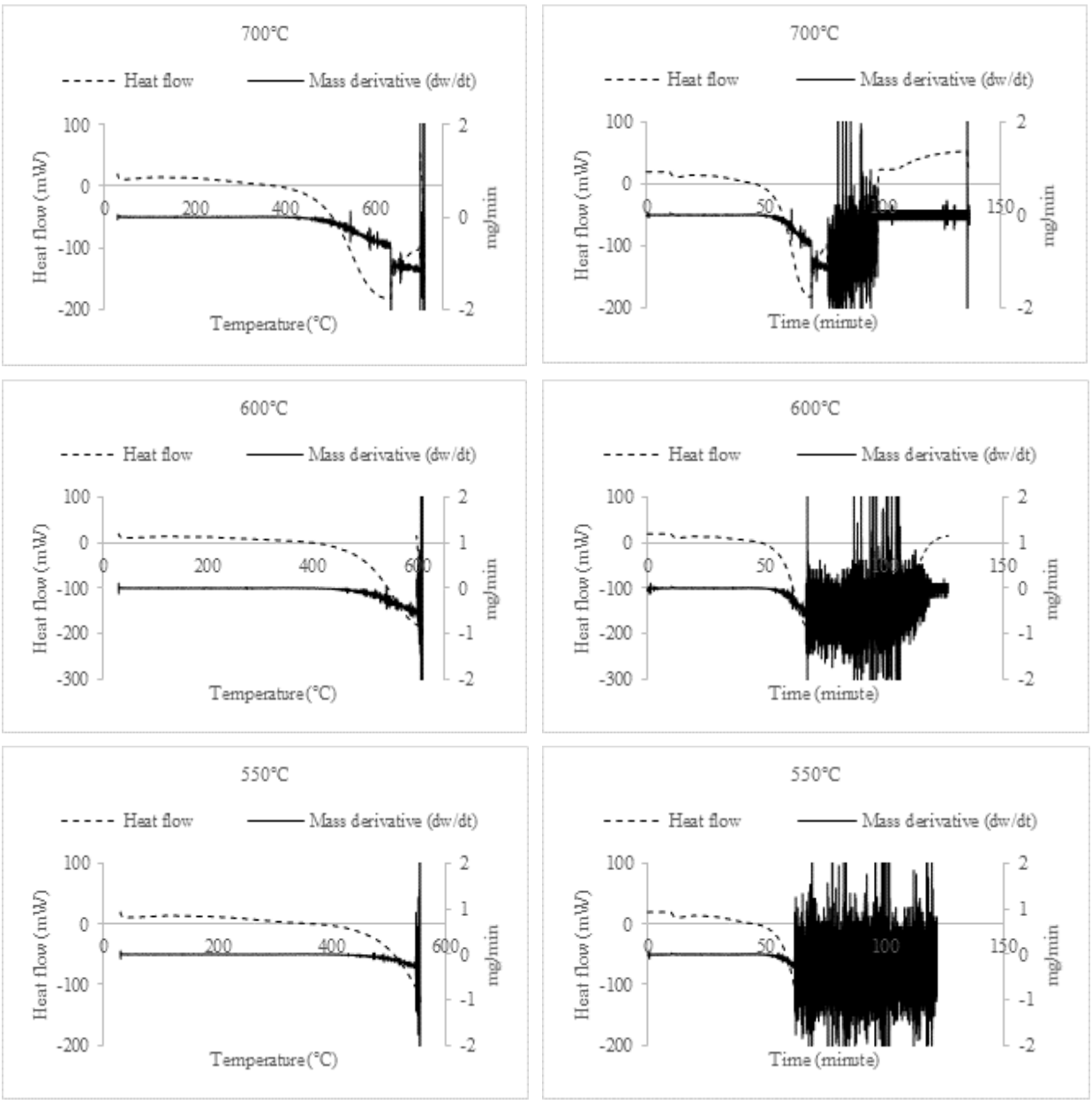

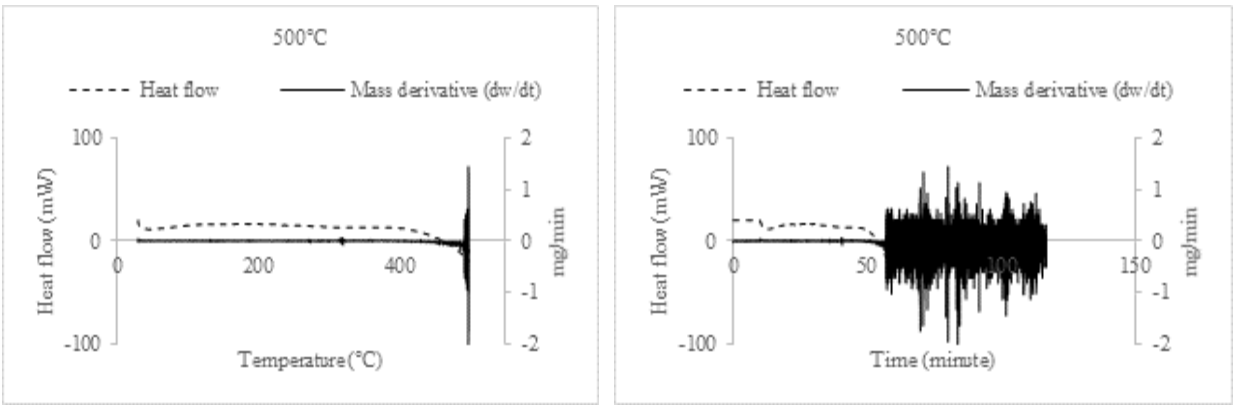

Figure 21: Heat flow and mass derivative of sample "550℃-24h-Spent" for combustion at different temperatures (700℃, 600℃, 550℃, and 500℃).

In Figure 21, heat flow and differential thermogravimetry data over temperature and time are provided for sample "550℃-24h-Spent" for oxidation reactions with air at four different temperatures (700℃, 600℃, 550℃, and 500℃). The heat flow and differential thermogravimetry data suggest that the exothermic reaction started at around 400℃. Similar behavior also has been noticed for the previous experiments. For the reaction up to 700℃, the curve shows the possibility of burning of different types of cokes with different characteristics. Overlap in the DSC signal also has been observed which suggest layered deposition of coke. So, the catalyst reacted at 550℃ promotes deposition of much varieties of coke than the higher temperature reaction. The reactions at lower temperatures could not develop well to have a clear insight.

Sample: "750℃-5h-Spent"

The Figure 22 illustrates graphs for reaction experiments of sample "750℃-5h-Spent" with air at four different temperatures (700℃, 600℃, 550℃, and 500℃). The heat flow profile and derivative of mass reduction curves are provided over temperature. The behavior of curves is almost similar with that of sample "750℃-24h-Spent".

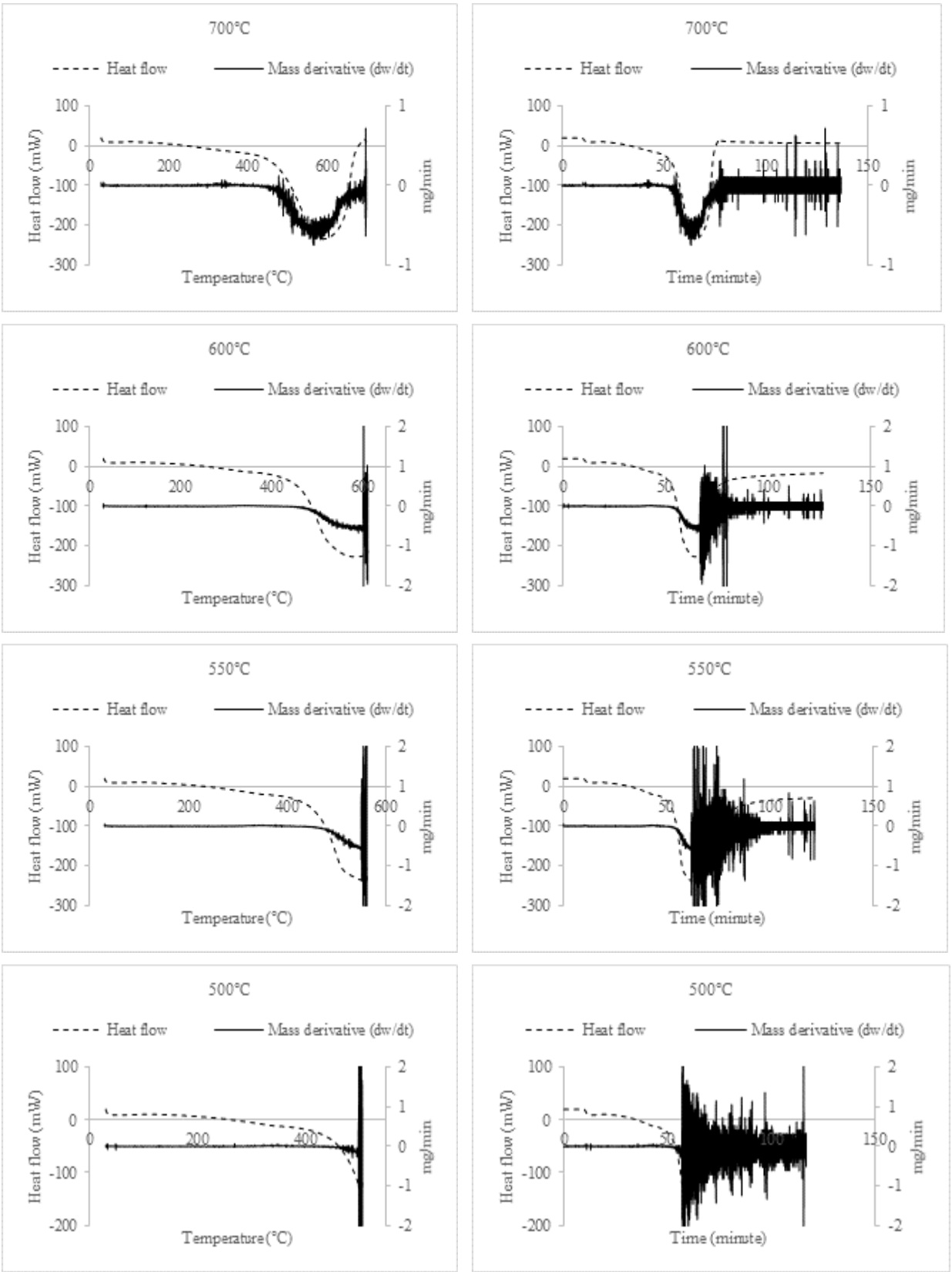

Figure 22: Heat flow and mass derivative of sample "750℃-5h-Spent" for combustion at different temperatures (700℃, 600℃, 550℃, and 500℃).

Sample: "550℃-5h-Spent"

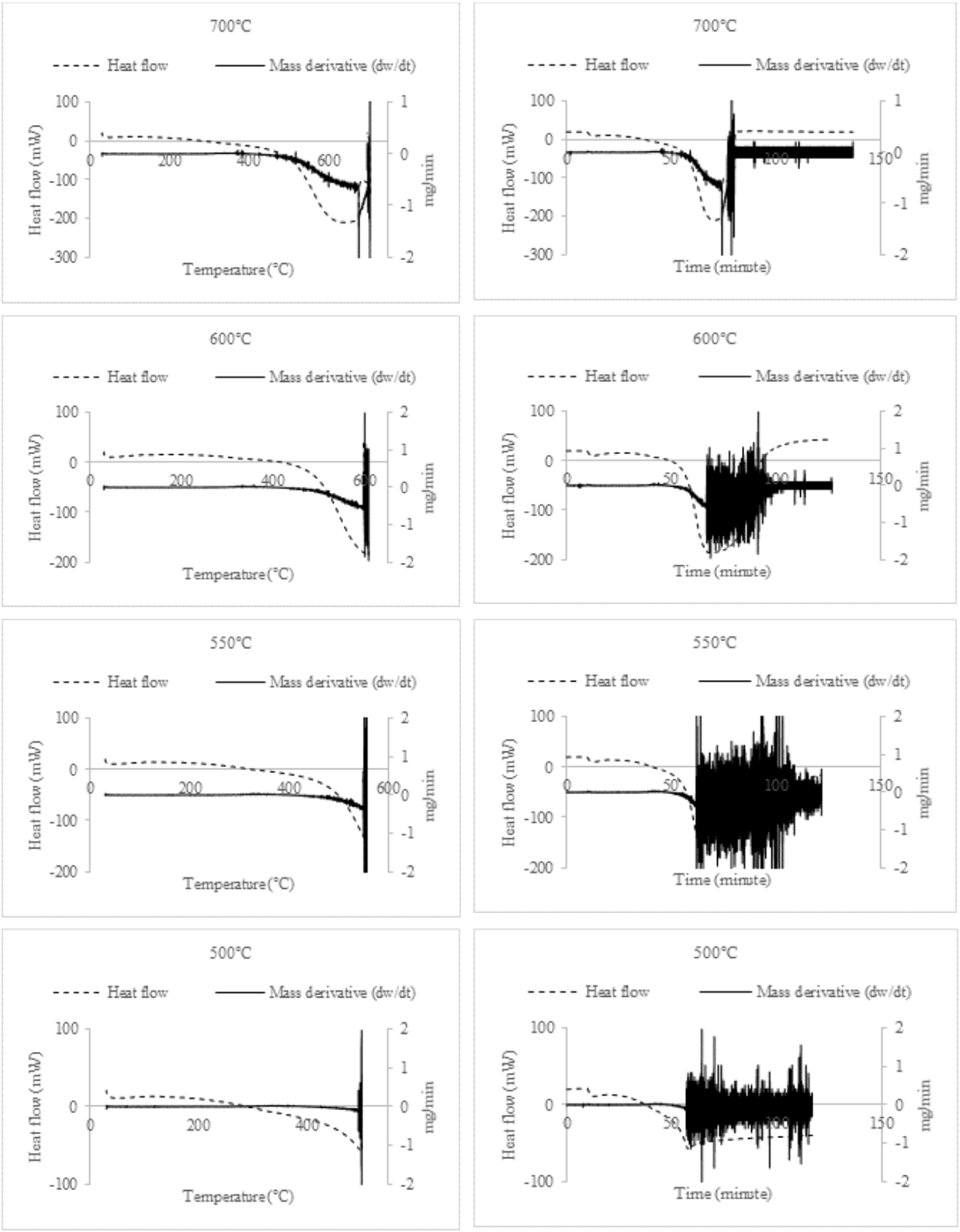

Figure 23: Heat flow and mass derivative of sample "550℃-5h-Spent" for combustion at different temperatures (700℃, 600℃, 550℃, and 500℃).

In Figure 23 heat flow and differential thermogravimetry data are provided with respect to temperature and time of sample “550℃-5h-Spent” for reaction with air up to four different temperatures (700℃, 600℃, 550℃, and 500℃). For the reaction up to 700℃, the exothermic reaction starts at around 400℃. An overlap in the exothermic peak has been noticed. Comparing with the sample “550℃-24h-Spent”, a smaller number of peaks is observed. The main difference between the two sample was duration of reaction cycle, one was of five hours and other of 24 hours. So, the duration of reaction cycle might influence the variety of species of the deposited coke. For other lower temperature reactions, the curves did not develop well to have a clear understanding.

4.2.3 DSC-DTG analysis of pyrolysis reaction with nitrogen

In dry reforming of methane reaction carbon dioxide reacts with methane but the reaction does not occur directly between methane and carbon dioxide. In the process methane and carbon dioxide are exposed to catalyst. Methane is oxidized on the catalyst and converted to syngas and later the catalyst is deoxidized with carbon dioxide. So the catalyst is used as oxygen carrier (Löfberg, Guerrero-Caballero, et al., 2017). Conversion of methane is influential and slower process than carbon dioxide conversion process. Therefore, there is possibility of accumulation of hydrogen containing volatile materials together with coke (Dębek et al., 2015). As a result, to analyze the presence of volatiles bearing hydrogen, pyrolysis reaction in the nitrogen atmosphere was investigated.

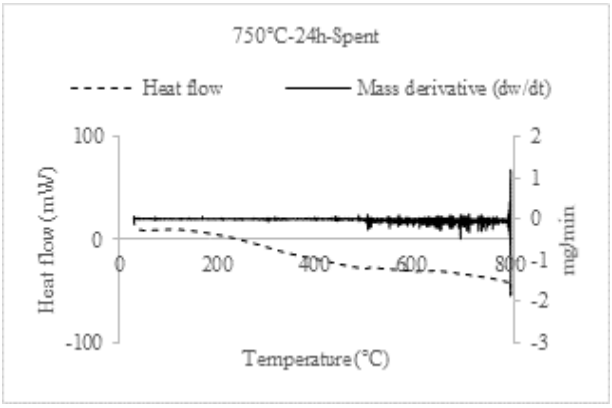

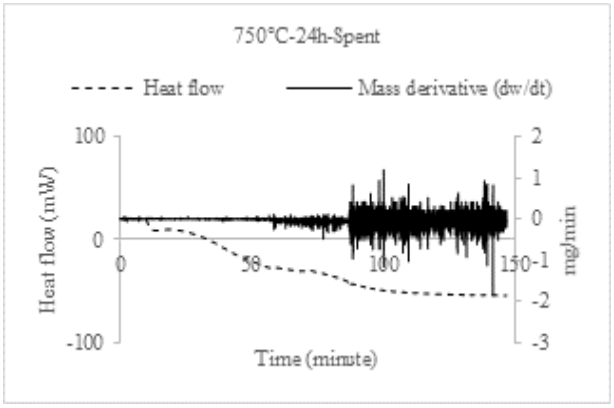

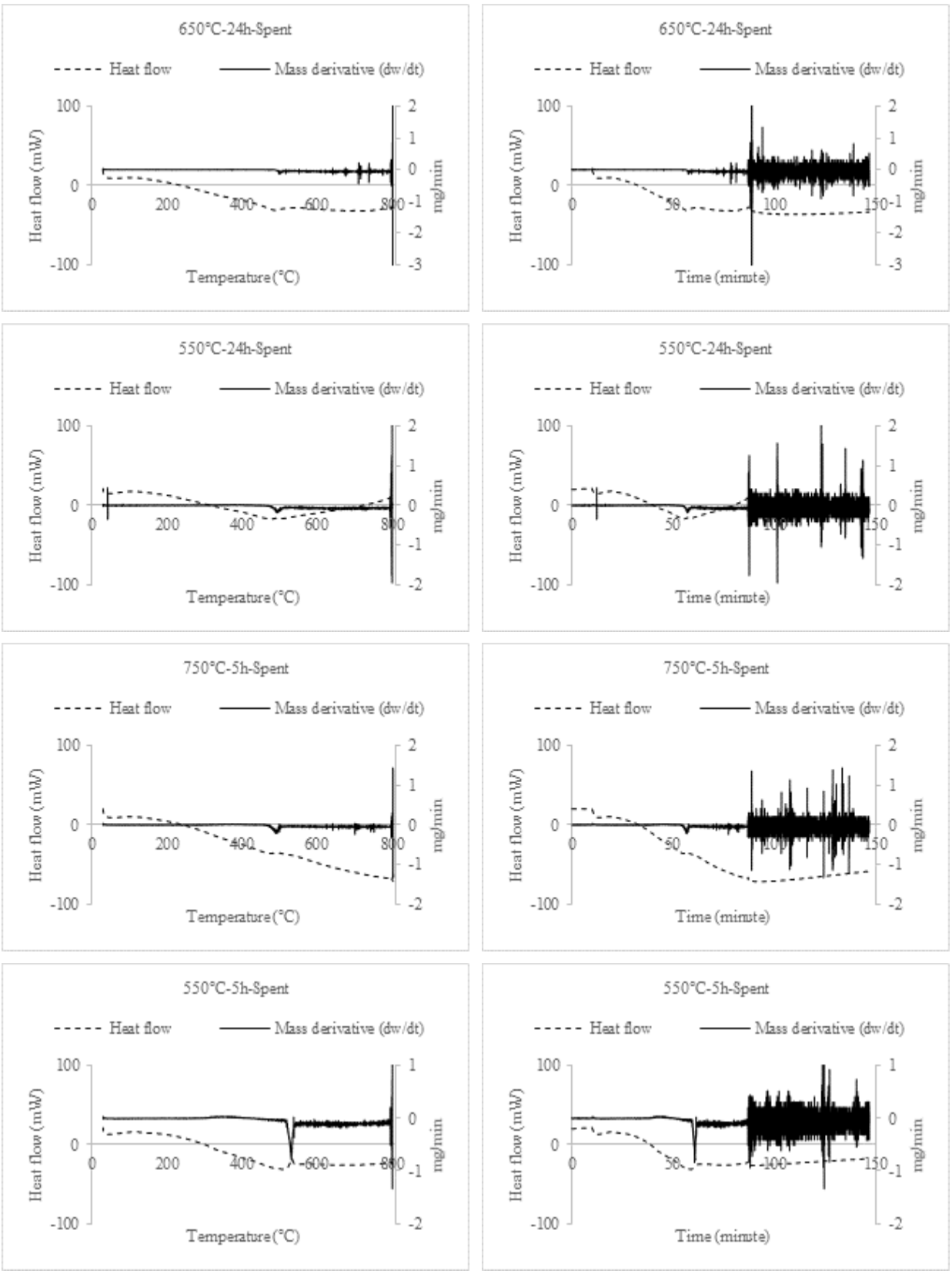

Figure 24: Heat flow and mass derivative of pyrolysis reaction with nitrogen for all samples.

In Figure 24 heat flow and differential of thermogravimetry data are provided in terms of temperature and time of all samples for pyrolysis reaction with nitrogen. The heating rate was 10℃ per minute. The samples were heated up to 800℃ and kept isothermal for one hour. For all samples it can be noticed from the graph that at around 300℃ it showed a start of an exothermic process. The samples that were used in high temperature DRM reaction (650℃, 750℃) illustrates an increasing pattern in heat flow in pyrolysis reaction. But the trend of the heat flow curve indicates that further increase in temperature was required to keep the pyrolysis reaction to go further. The catalyst samples used in low temperature (550℃) DRM reaction, showed different characteristics. At around 500℃ exothermic peak seems to be reached. Overlap in the heat flow data also has been noticed. This indicates hydrogen deposition with volatile materials in layered structure. It also has been noticed that at lower temperature DRM reaction species with lower bond energy was deposited.

4.2.4 DSC-DTG analysis of gasification of coke with carbon dioxide

The Figure 25 represents heat flow and differential thermogravimetry over temperature and time of all samples for gasification of coke with carbon dioxide. The samples were heated with a heating rate of 10℃ per minute from 40℃ to 800℃ and kept isothermal at end temperature for one hour. The heat flow data depicts that for all samples the endothermic reaction started over 500℃. At around 600℃ the peak is reached. After the endothermic reaction the baseline went little bit higher comparing to pre-reaction baseline. This indicates that after the endothermic reaction the heat capacity of the post reaction component increased a bit.

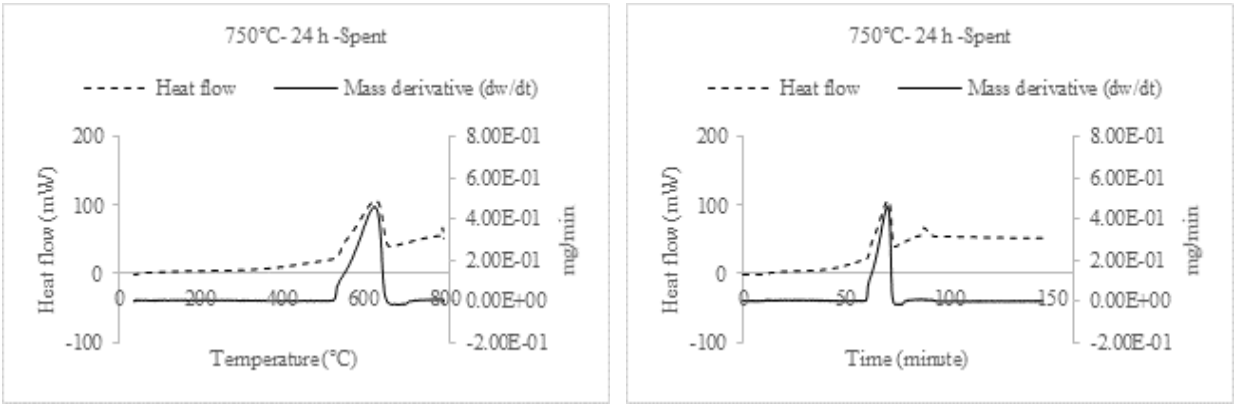

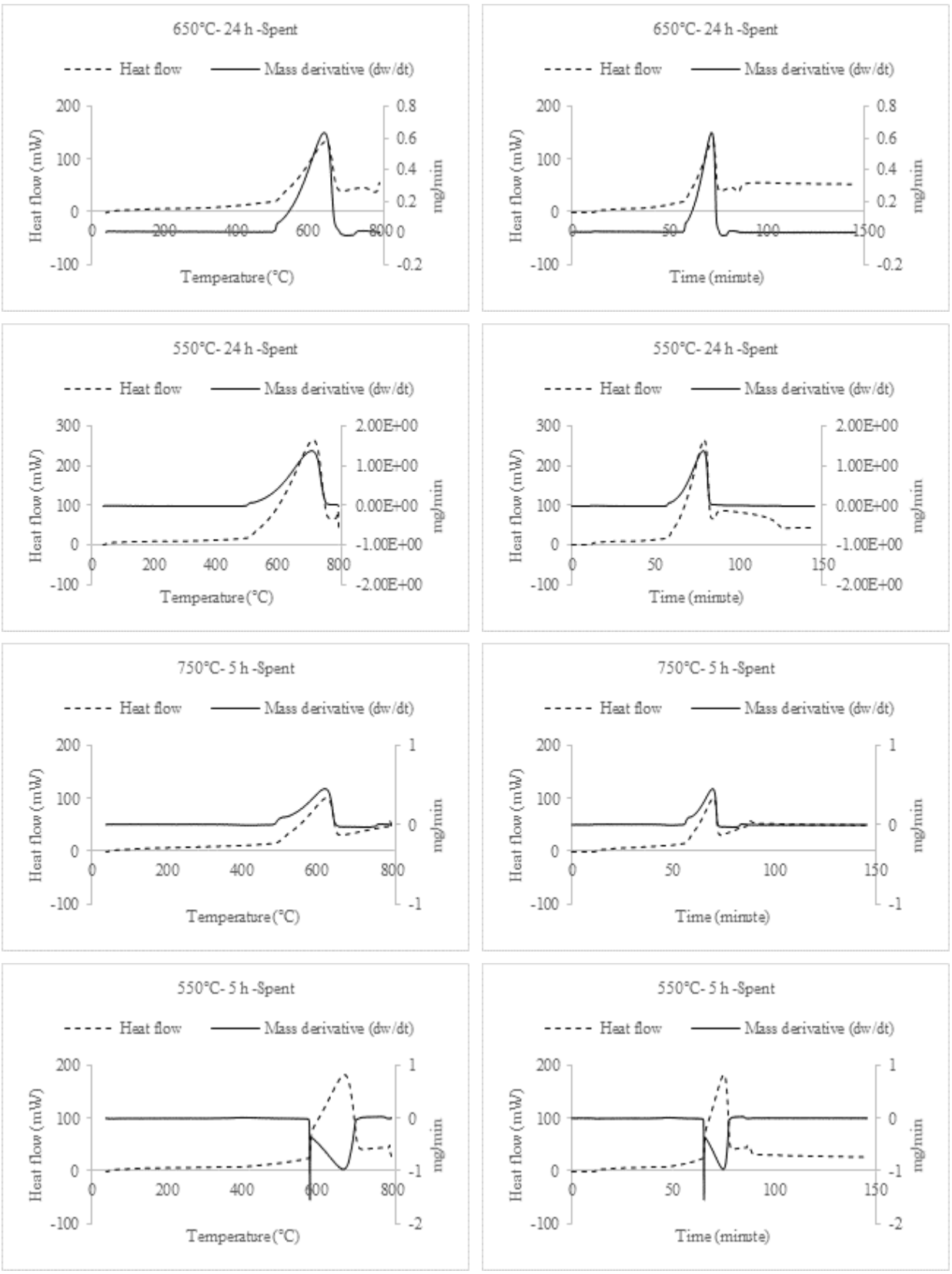

Figure 25: Heat flow and mass derivative of gasification of coke with carbon dioxide of all samples.

4.3 Kinetic parameter estimation by model fitting

The idea behind the kinetic model is to compute kinetic parameters of reaction kinetics. In kinetic model simulation, it was assumed that pseudo components are thermally degraded through various reaction such as: combustion with air, pyrolysis with nitrogen, and gasification with carbon dioxide. In addition, it was also assumed that the conversion of pseudo components follows first order reaction that they are independent of each other. The pseudo component was calculated using Euler's method. Least square method was used to determine pre-exponential factor, activation energy, and mass fraction of each pseudo component. Generalized Reduced Gradient (GRG) nonlinear algorithm was used in solver tool of Microsoft Excel.

4.3.1 Kinetic model fitting of combustion with air up to 800℃

In this section the Figure 26 shows model fitting together with experimental data of all samples for combustion with air up to 800℃ with retention at this isothermal condition for one hour and heating rate of 10℃ per minute. From the Figure 26, it can be noticed that the curves fitting is quite precise, and the model can almost accurately describe thermal behavior of the samples. The kinetic parameters of the reactions were determined through model fitting. Table 10 provides activation energy, reaction rate constant, and mass fraction of each pseudo component.

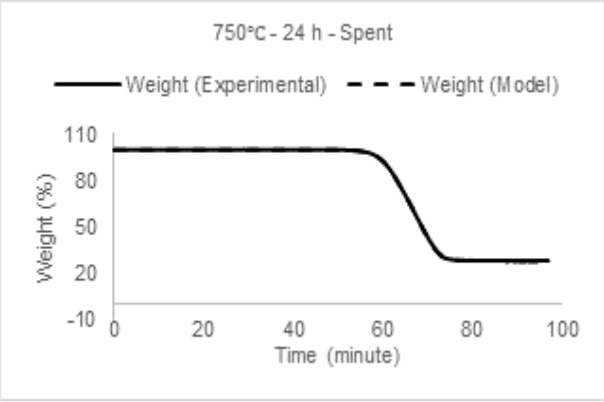

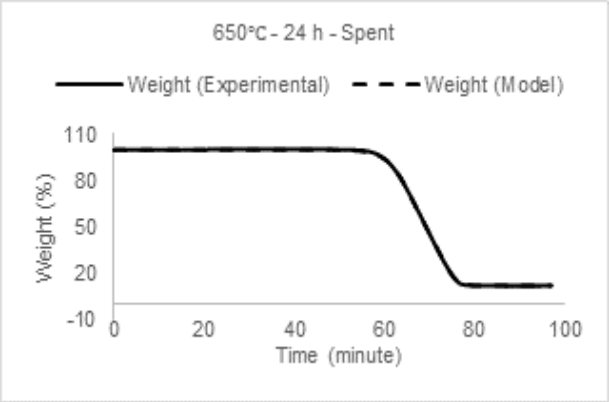

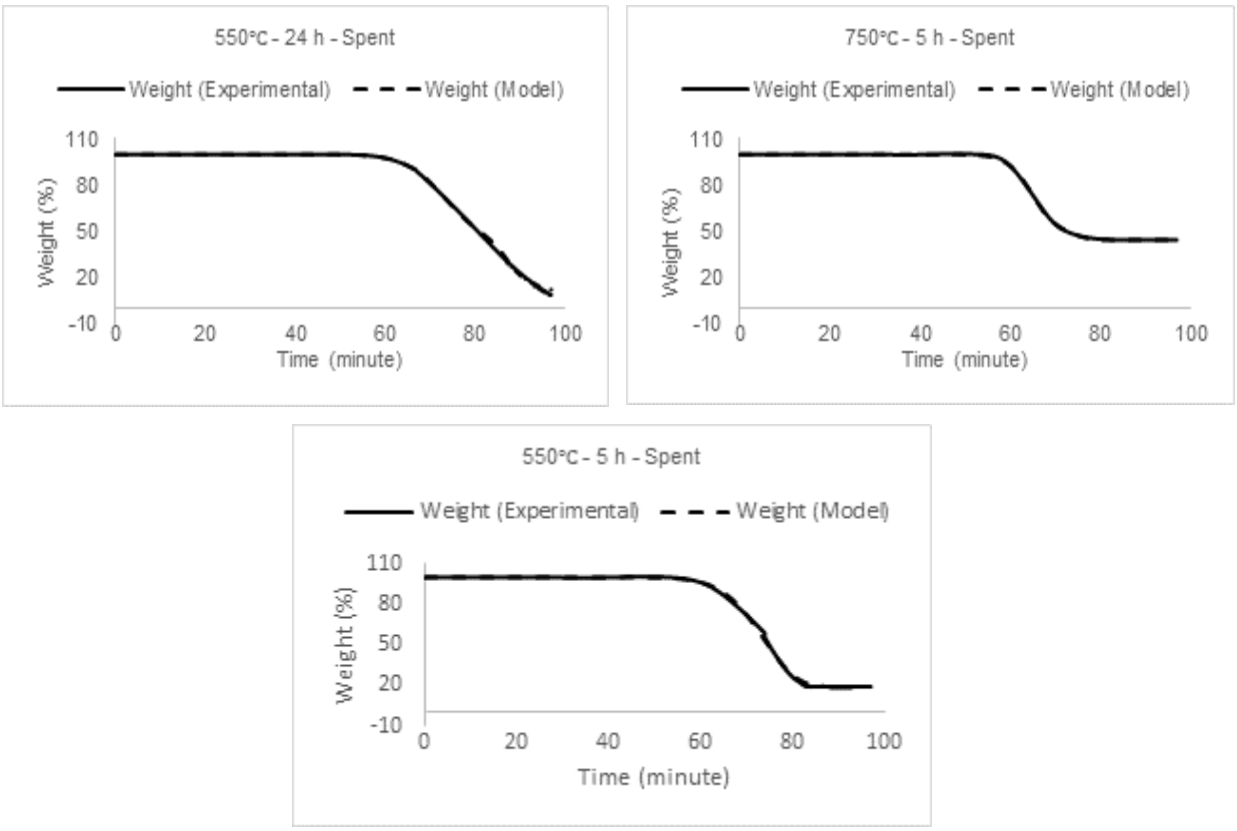

Figure 26: Model fitting for combustion reaction with air up to 800℃.

Table 10: Kinetic parameters of combustion reaction with air up to 800℃ of all samples.

Sample name	750℃-24h-Spent	650℃-24h-Spent	550℃-24h-Spent	750℃-5h-Spent	550℃-5h-Spent
Component 1 (%)	11.52	40.19	47.345	33.63	80.913
K (1/min)	1.36E-10	1.90E-08	3.50E-07	3.18E-08	4.80E-07
Ea (kJ/mole)	54508.17	39024.2	27604.41	38239.85	26514.73
Component 2 (%)	60.42	47.963	44.05	22.06	0
K (1/min)	1.94E-08	2.59E-12	6.87E-16	1.46E-07	0
Ea (kJ/mole)	36770.314	54362	61549.65	30861.62	0

In Figure 26, catalyst used in high temperature DRM reaction, exhibit better fit than the catalyst used in low temperature DRM reaction. From Table 10, in all reactions two types of pseudo components were found except for the sample “550℃-5h-Spent” where only one pseudo component was deposited.

4.3.2 Kinetic model fitting of combustion with air at different temperatures

Sample: "750℃-24h-Spent"

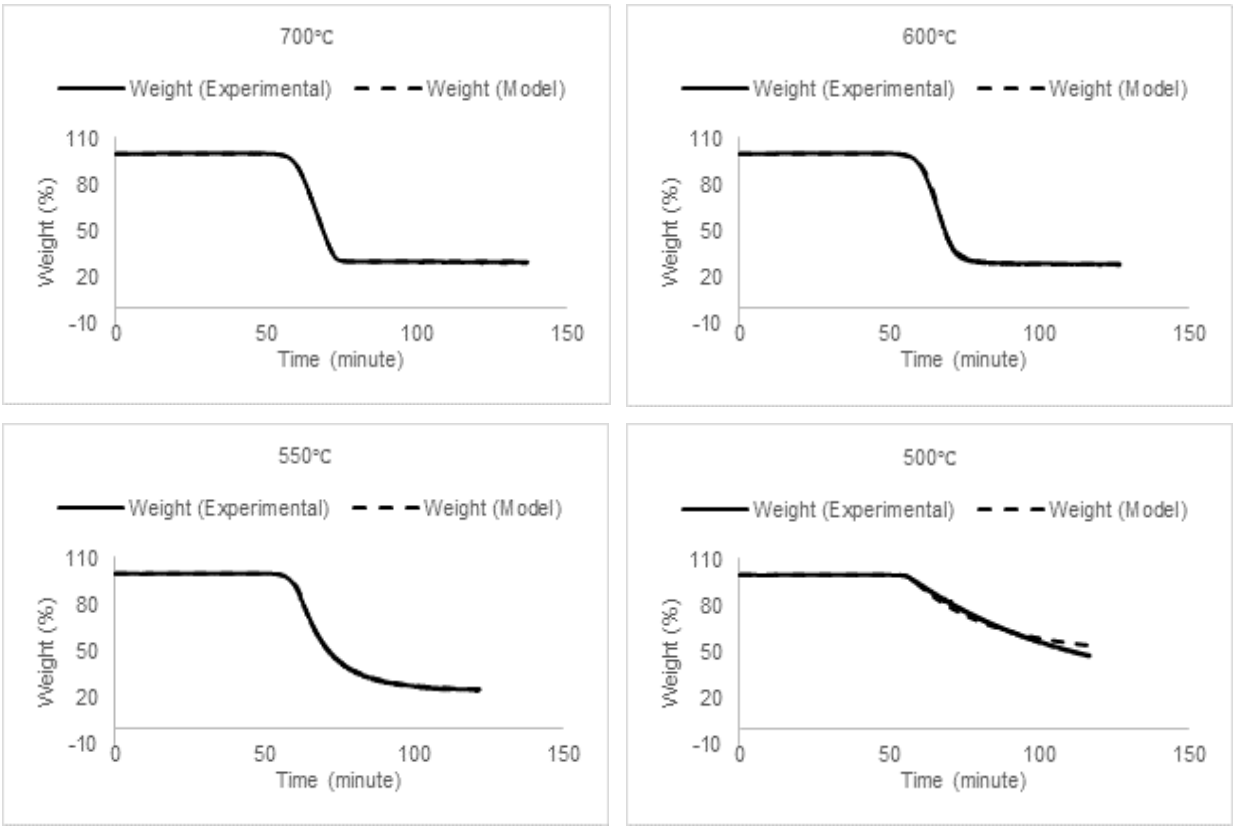

Figure 27: Model fitting of combustion with air at 550℃, 550℃, 600℃, and 700℃ of sample "750℃-24h-Spent".

Table 11: Kinetic parameters of combustion reaction with air at different temperatures of sample "750℃-24h-Spent".

750℃-24h-Spent	700℃	600℃	550℃	500℃
Component 1 (%)	12.79	71.53	33.45	52.36
K (1/min)	2.01E-10	2.35E-08	1.38E-09	2.33E-14
Ea (kJ/mole)	53464.92	37002.15	44841.86	78148.34
Component 2 (%)	57.36	0	41.81	0
K (1/min)	1.11E-08	0	4.04E-10	0
Ea (kJ/mole)	38034.3	0	47933.89	0

Sample: "650℃-24h-Spent"

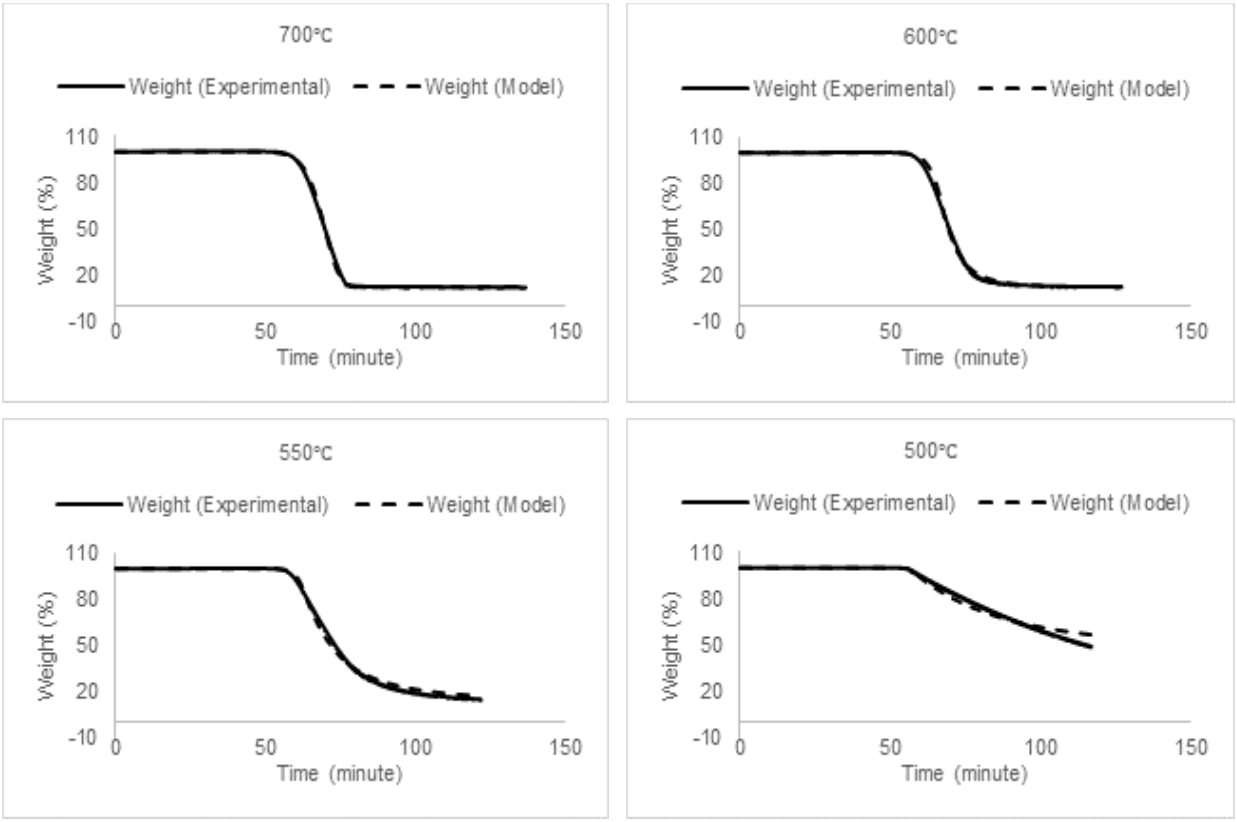

Figure 28: Model fitting of combustion with air at 550℃, 550℃, 600℃, and 700℃ of sample "650℃-24h-Spent".

Table 12: Kinetic parameters of combustion reaction with air at different temperatures of sample "650℃-24h-Spent".

650℃-24h-Spent	700℃	600℃	550℃	500℃
Component 1 (%)	28.032	59.948	39.358	51.014
K (1/min)	1.05E-08	3.68E-09	3.14E-11	1.53E-14
Ea (kJ/mole)	41077.7	40165.73	53483.24	78724.52
Component 2 (%)	59.704	27.746	45.952	0
K (1/min)	1.75E-10	1.63E-10	2.60E-11	0
Ea (kJ/mole)	45413	47324.42	53956.06	0

Figure 27-28 illustrate model fitting for reaction experiments of sample "750℃-24h-Spent" and "650℃-24h-Spent" respectively with air at four different temperatures (700℃, 600℃, 550℃, and 500℃). The graphs demonstrate that model fitting for the reaction experiments at 700℃, 600℃, and 550℃ temperatures are quite well comparing to that of 500℃. Table 11-12 depict the kinetic parameters of the reactions such as: activation energy, reaction rate constant, and mass fraction of each pseudo component for sample "750℃-24h-Spent" and "650℃-24h-Spent" respectively. Table 11 shows that the kinetic model simulation provides

with two pseudo components for combustion reactions of 700℃ and 550℃ temperature while that for the reaction of 600℃ and 500℃ temperature provides with only one pseudo component. In Table 12 the kinetic model simulation provides with two pseudo components for the combustion reactions of all temperatures except 500℃. Though the kinetic model provides two pseudo components, the activation energy value for both components are almost similar for combustion reactions at 700℃, 600℃, and 550℃.

Sample: "550℃-24h-Spent"

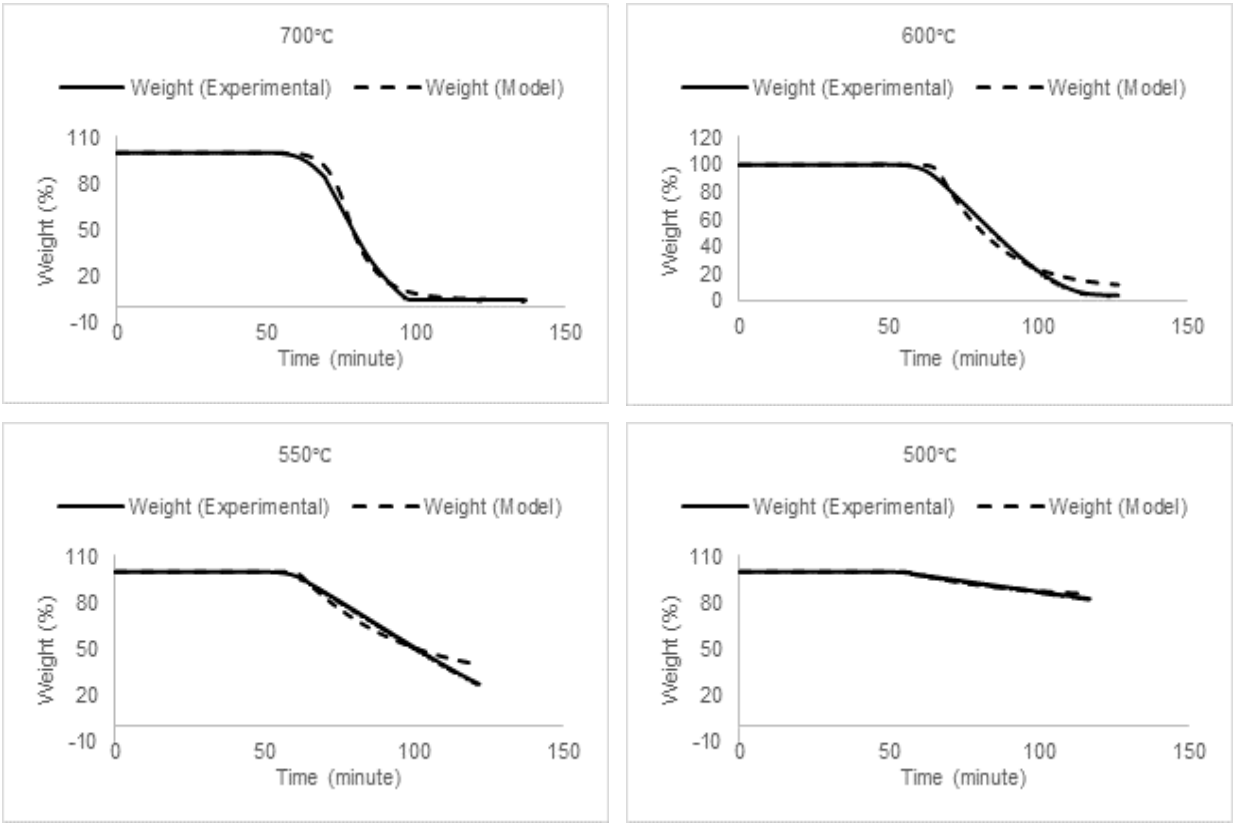

Figure 29: Model fitting of combustion with air at 550℃, 550℃, 600℃, and 700℃ of sample "550℃-24h-Spent".

Table 13: Kinetic parameters of combustion reaction with air at different temperatures of sample "550℃-24h-Spent".

550℃-24h-Spent	700℃	600℃	550℃	500℃
Component 1 (%)	95.633	95.654	72.88	17.495
K (1/min)	2.77E-09	1.82E-16	2.35E-15	2.82E-15
Ea (kJ/mole)	35476.77	75815.3	75247.3	84138.49
Component 2 (%)	0	0	0	0
K (1/min)	0	0	0	0
Ea (kJ/mole)	0	0	0	0

Figure 29 illustrates model fitting for reaction experiments of sample “550℃-24h-Spent” with air at four different temperatures (700℃, 600℃, 550℃, and 500℃). The graph illustrates that model fitting of the reaction experiments are not quite well comparing to previous model fittings. It might be the reason of low temperature DRM reaction which caused accumulation of various species. Table 13 depicts the kinetic parameters of the reactions such as: activation energy, reaction rate constant, and mass fraction of each pseudo component. The kinetic model simulation provides with one pseudo component for all the reactions. The activation energy of pseudo components seems to decrease with the increase in isothermal combustion temperature.

Sample: “750℃-5h-Spent”

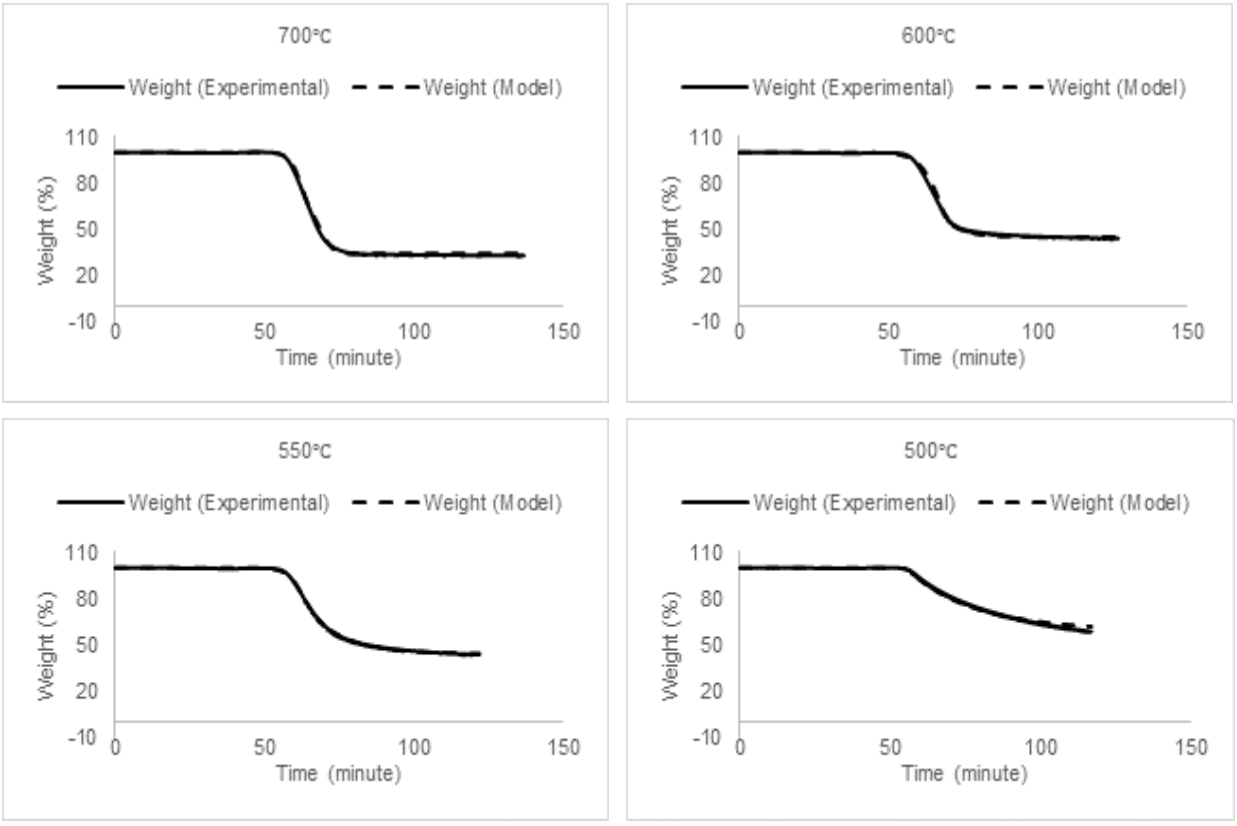

Figure 30: Model fitting of combustion with air at 550℃, 550℃, 600℃, and 700℃ of sample “750℃-5h-Spent”.

Table 14: Kinetic parameters of combustion reaction with air at different temperatures of sample "750℃-5h-Spent".

750℃-5h-Spent	700℃	600℃	550℃	500℃
Component 1 (%)	22.819	34.218	56.063	41.418
K (1/min)	1.36E-10	5.20E-06	2.53E-07	2.40E-11
Ea (kJ/mole)	54508.17	23936.85	31768.25	59297.41
Component 2 (%)	43.006	20.803	0	0
K (1/min)	1.94E-08	1.34E-11	0	0
Ea (kJ/mole)	36770.31	54508.17	0	0

Figure 30 illustrates model fitting for reaction experiments of sample "750℃-5h-Spent" with air at four different temperatures (700℃, 600℃, 550℃, and 500℃). The graph demonstrates that model fitting for the reaction experiments at 700℃, 600℃, and 550℃ temperatures are quite well comparing to that of 500℃. Table 14 depicts kinetic parameters of all reaction experiments of the sample. It indicates that the kinetic model simulation provides with two pseudo components for the combustion reactions of 700℃ and 600℃ temperatures while that is for 550℃ and 500℃ provides with only one pseudo component.

Sample: "550℃-5h-Spent"

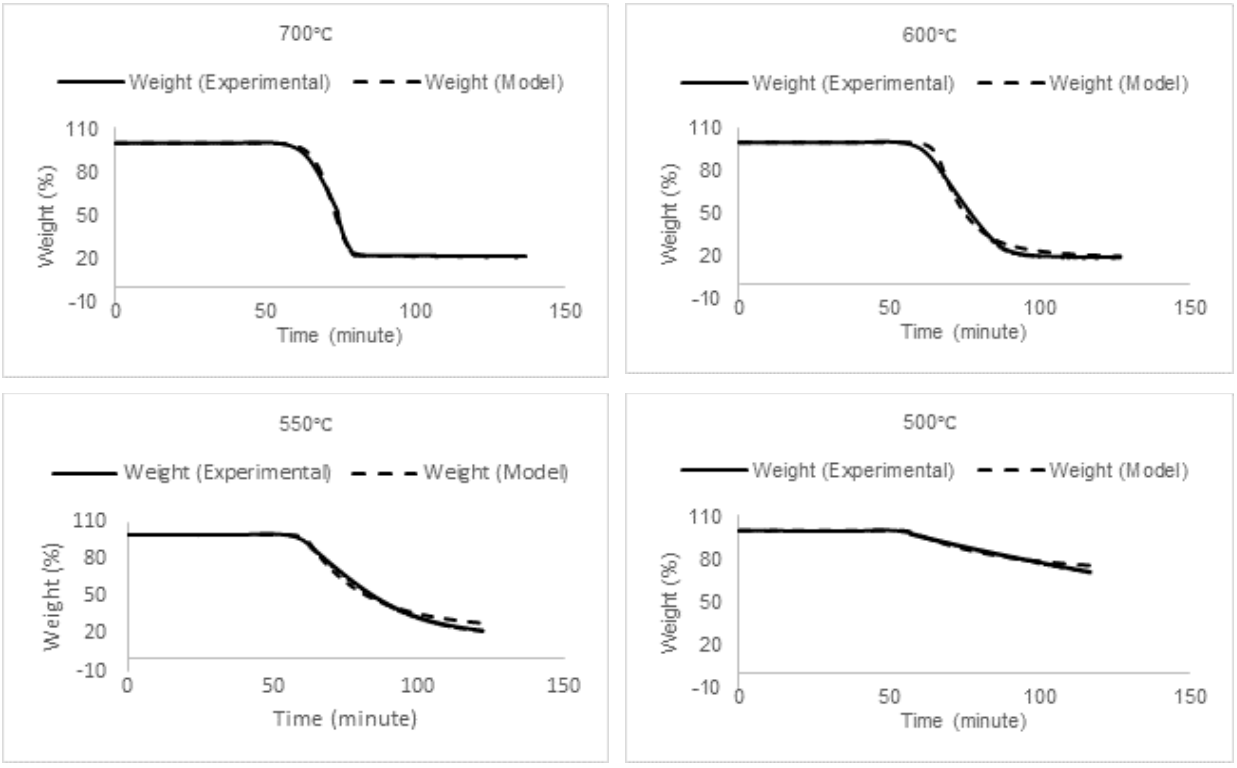

Figure 31: Model fitting of combustion with air at 550℃, 550℃, 600℃, and 700℃ of sample "550℃-5h-Spent".

Table 15: Kinetic parameters of combustion reaction with air at different temperatures of sample "550℃-5h-Spent".

550℃-5h-Spent	700℃	600℃	550℃	500℃
Component 1 (%)	78.606	81.145	77.07	28.87
K (1/min)	9.00E-09	2.35E-12	3.77E-12	5.23E-16
Ea (kJ/mole)	36000	55855.92	56572.61	88512.65
Component 2 (%)	0	0	0	0
K (1/min)	0	0	0	0
Ea (kJ/mole)	0	0	0	0

Figure 31 illustrates model fitting for reaction experiments of sample "550℃-5h-Spent" with air at four different temperatures (700℃, 600℃, 550℃, and 500℃). The graph illustrates that model fitting of the reaction experiments are not quite well comparing to previous model fitting. It might be the same reason that we have seen for the sample "550℃-24h-Spent" that low temperature DRM reaction caused accumulation of various species. Table 15 depicts the kinetic parameters of the reactions such as: activation energy, reaction rate constant, and mass fraction of each pseudo component. The kinetic model simulation provides with one pseudo component for all the reactions.

4.3.3 Kinetic model fitting of pyrolysis reaction with nitrogen

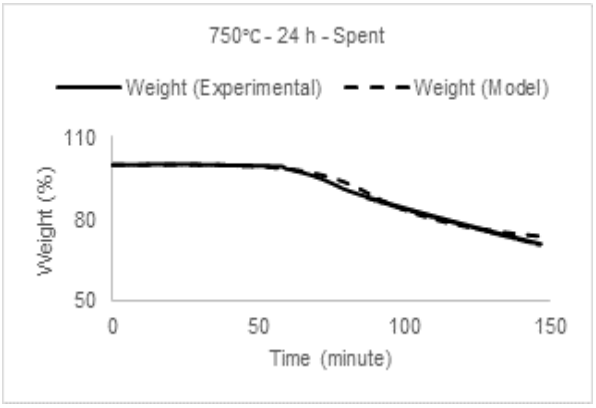

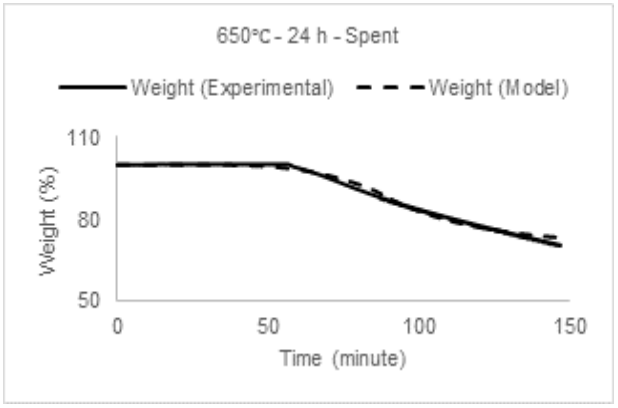

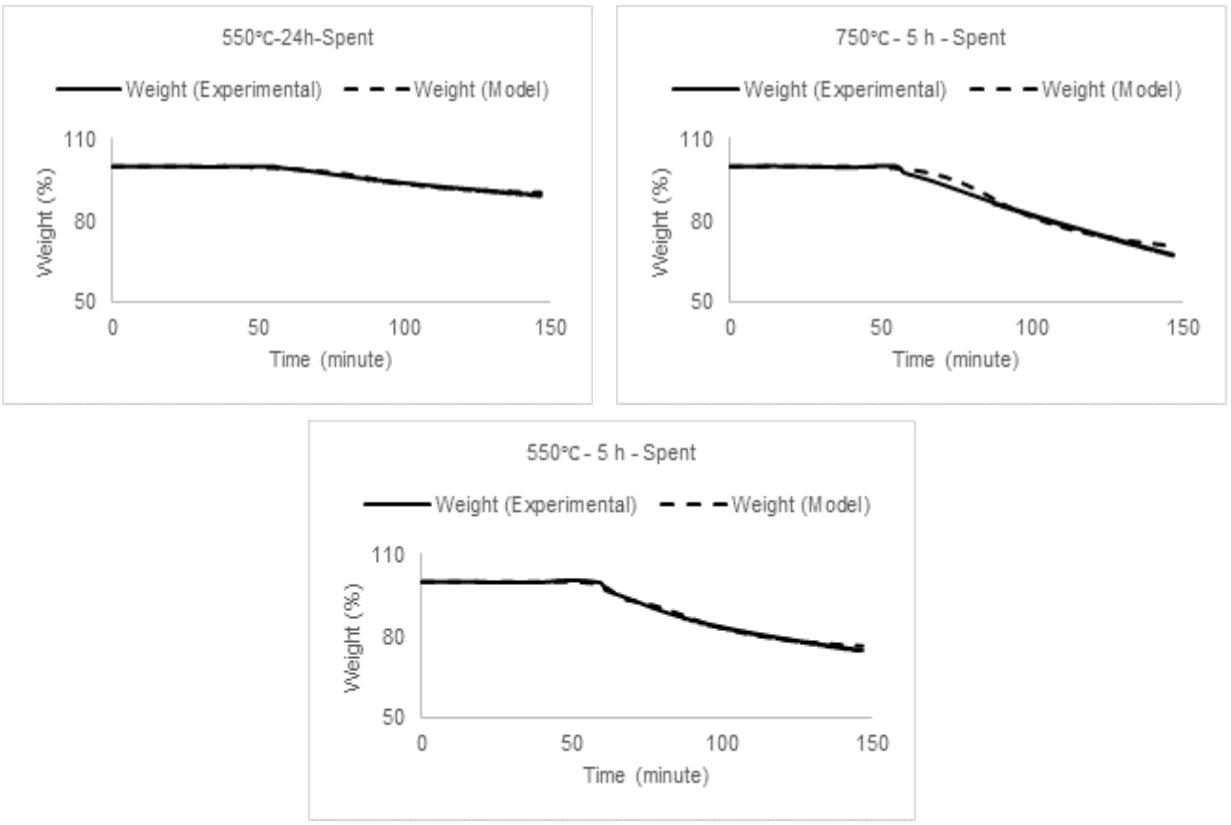

Figure 32: Model fitting of pyrolysis with nitrogen for all tested samples.

Table 16: Kinetic parameters of pyrolysis reaction with nitrogen of samples.

Sample name	750℃-24h-Spent	650℃-24h-Spent	550℃-24h-Spent	750℃-5h-Spent	550℃-5h-Spent
Component 1 (%)	17.206	21.816	6.494	32.354	5.218
K (1/min)	6.57E-07	3.24E-04	1.01E-3	6.24E-05	2.45E-10
Ea (kJ/mole)	19928.22	8529.067	6434.632	11484.75	51759.5
Component 2 (%)	11.762	7.566	4.07	0	19.887
K (1/min)	7.57E-4	2.87E-17	3.87E-09	0	2.19E-05
Ea (kJ/mole)	6963.166	64158.96	29535.42	0	13649.82

Figure 32 illustrates kinetic model fitting of all samples for pyrolysis reaction with nitrogen. The heating rate was 10℃ per minute. The samples were heated up to 800℃ and kept isothermal for one hour. For all samples it can be noticed from the graph that the model fitting was quite accurate. From the mass degradation trend, it is noticed that these patterns could go further in pyrolysis reaction. But further increase in temperature was required to keep the pyrolysis reaction go further. Table 16 represents kinetic parameters of all pyrolysis reaction found by kinetic simulation.

4.3.4 Kinetic model fitting of gasification of coke with carbon dioxide

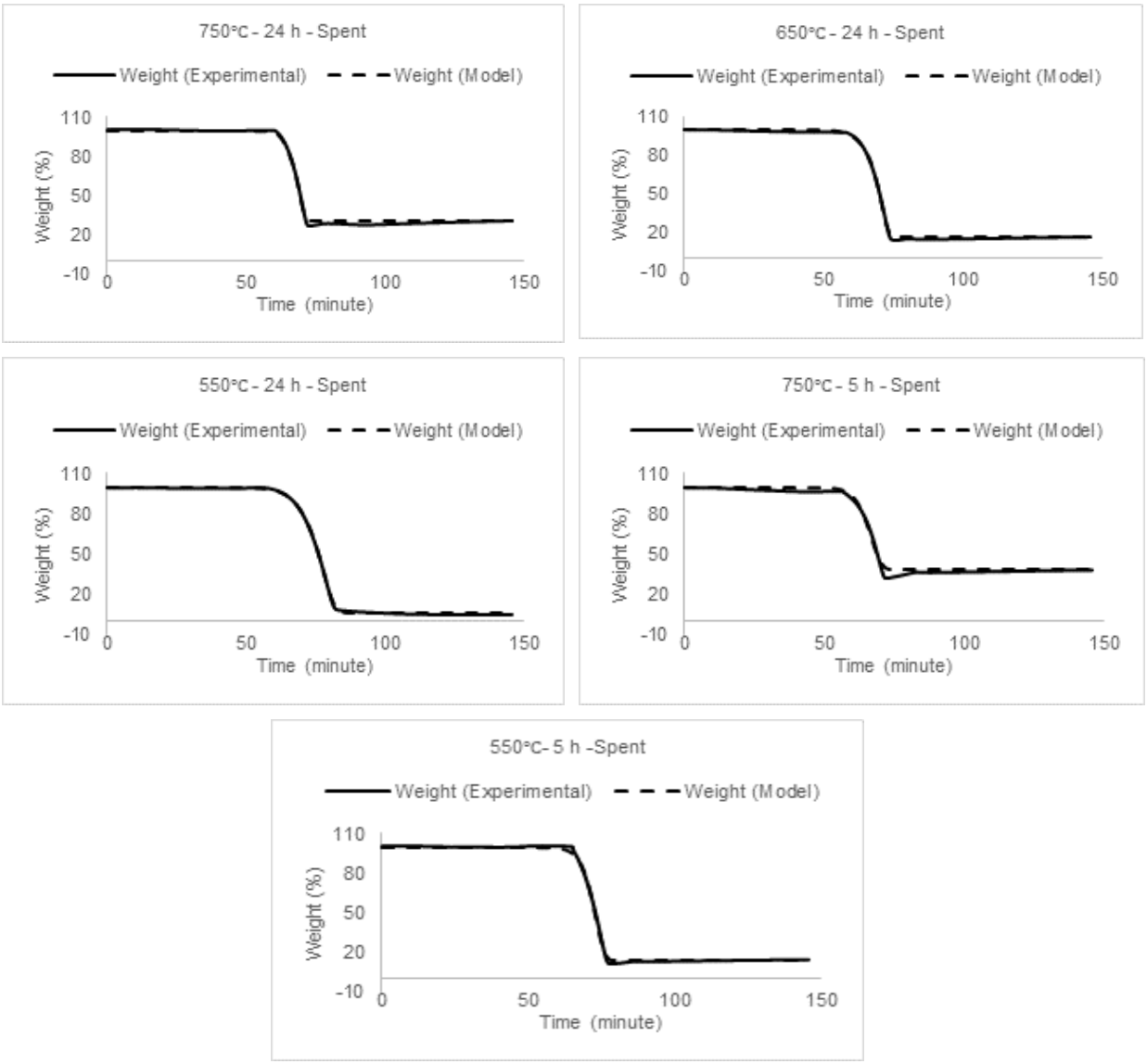

Figure 33: Model fitting of gasification of coke with carbon dioxide of all samples.

Table 17: Kinetic parameters of gasification reaction with carbon dioxide of samples.

Sample name	750℃-24h-Spent	650℃-24h-Spent	550℃-24h-Spent	750℃-5h-Spent	550℃-5h-Spent
Component 1 (%)	11.817	24.166	67.317	26.212	85.797
K (1/min)	3.42E-15	3.25E-07	6.79E-08	6.70E-09	1.38E-12
Ea (kJ/mole)	79767.82	31827.56	30671.56	40917.72	56274.05
Component 2 (%)	57.045	60.113	27.195	36.026	0
K (1/min)	2.80E-16	1.39E-14	2.35E-16	7.05E-09	0
Ea (kJ/mole)	79225.37	68349.11	70625.58	40805.17	0

Figure 33 represents kinetic model fitting of all samples for gasification with carbon dioxide. The samples were heated with a heating rate of 10℃ per minute from 40℃ to 800℃ and kept isothermal at end temperature for one hour. The model fitting was quite accurate that it can be observed from the graph. Table 17 provides kinetic parameters of all gasification reaction with carbon dioxide found by kinetic simulation. Though in the Table 17 two pseudo components can be seen in majority cases, in higher temperature DRM reaction almost similar types of pseudo components are deposited as they have almost similar activation energy while at lower temperature different types of pseudo components are deposited.

4.3.5 Comparison of activation energy of combustion, gasification and pyrolysis

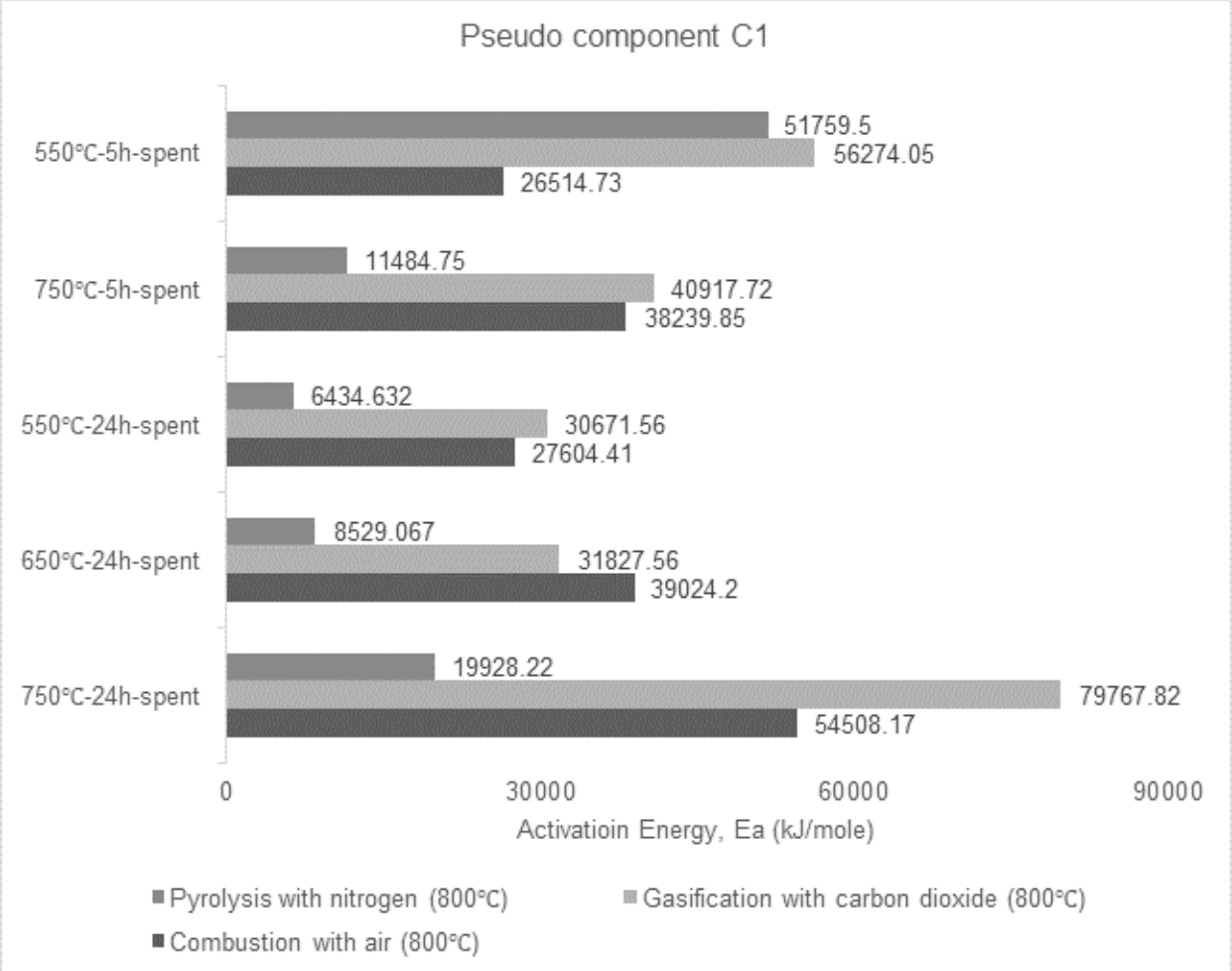

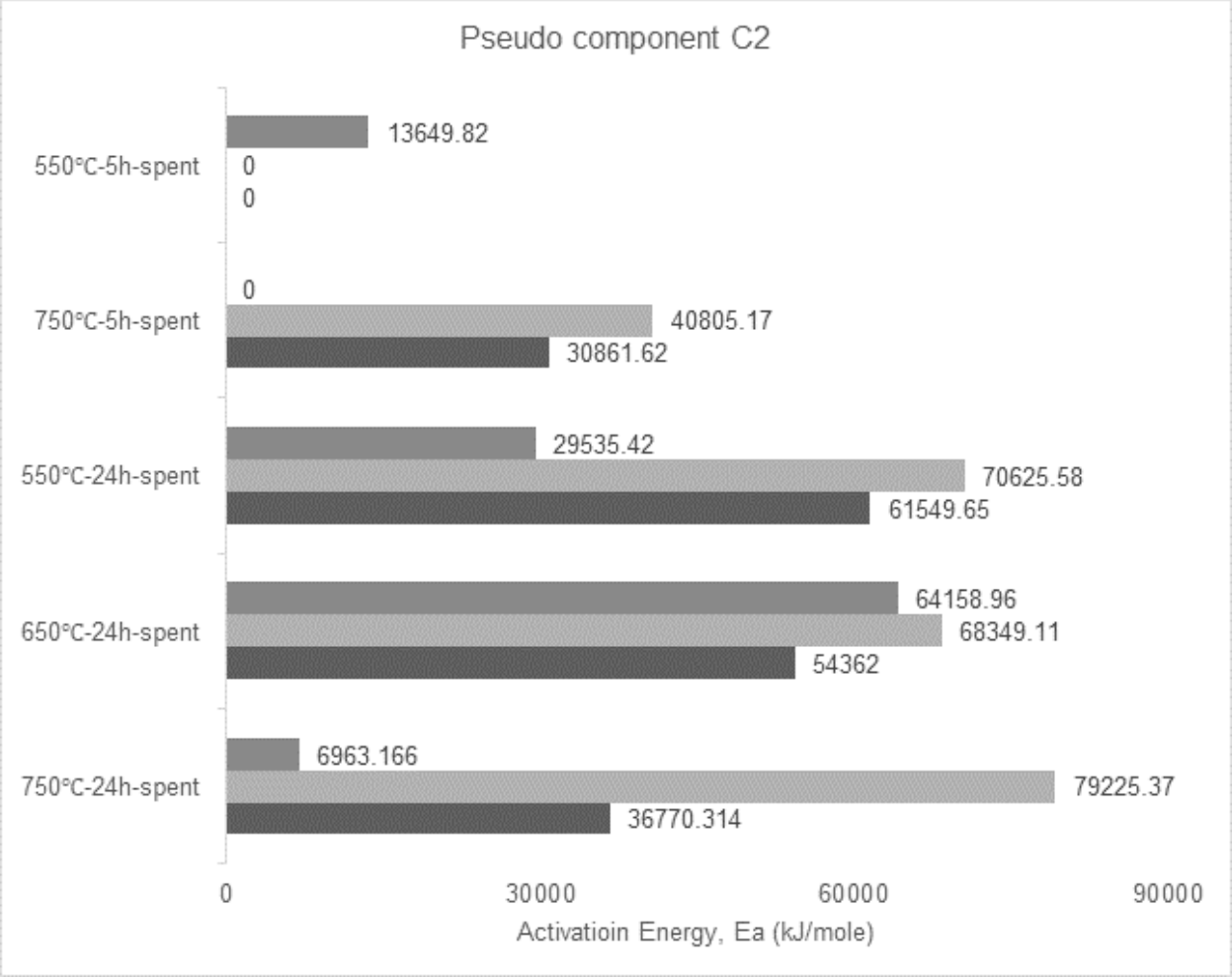

Figure 34: Activation energy of pseudo component C1 and C2 for combustion, gasification, and pyrolysis reaction.

The comparison of apparent activation energy of pseudo component C1 and C2 is presented in Figure 34 which depicts activation energy of pseudo component C1 and C2 of all the samples that had been analyzed in three different reaction processes namely: combustion with air, gasification with carbon dioxide, and pyrolysis with nitrogen. The pseudo component C1 represents the volatiles that were released at lower temperature of the reaction and pseudo component C2 represents volatiles that were released at comparatively higher temperature. In all the mentioned processes temperature was raised to 800℃. For gasification and pyrolysis process the samples were kept in isothermal condition for 60 minutes and in combustion reaction the isothermal retention time was 10 minutes.

The activation energy of pseudo components C1 and C2 is higher for almost all gasification reaction with carbon dioxide. It is a complex comparison and further analysis is required to have more clear insight.

Conclusion

As carbon dioxide and methane are the two major contributors of greenhouse gas emission, technology should be developed to have a check on the emission. Dry reforming of methane (DRM) is a potential option in this regard, as in DRM reaction, these gases are consumed to provide with synthesis gas. This technology provides the way for sustainable development together with environmental protection and efficient use of energy resources.

DRM is a chemical reaction that converts carbon dioxide and methane to syngas. This is an endothermic reaction which has optimum temperature range between 600℃ to 1000℃ to have desirable level of conversion. In DRM reaction the solid catalyst plays a vital role in this. It acts as oxygen carrier, producing syngas while exposure to methane and getting re-oxidized while exposure to carbon dioxide. But establishment of DRM technology is suffered by various drawbacks such as: high reaction temperature, formation of coke, and reduction in selectivity due to water gas shift reaction.

The objective of this study involved analyzing regeneration characteristics of Ni-based catalyst that was used for DRM reaction. For analysis purpose five types of samples were used in temperature condition ranging from 550℃ to 750℃ with different feed mixtures of gases (CH_4/CO_2/Ar = 1/1/8 and CH_4/CO_2/Ar = 1.5/1.5/7). Four types of experiments have been done such as: (a) combustion with air up to 800℃, where the temperature was raised from 30℃ to 800℃ at a rate of 10℃ per minute and kept in isothermal condition for 10 minutes, (b) combustion with air at different temperatures (700℃, 600℃, 550℃, and 500℃), where the temperature was raised from 30℃ to preferred temperature at a rate of 10℃ per minute and kept in isothermal condition for 60 minutes, (c) pyrolysis with nitrogen, where the temperature was raised from 30℃ to 800℃ at a rate of 10℃ per minute and kept in isothermal condition for 60 minutes, and (d) gasification of coke with carbon dioxide, where the temperature was raised from 40℃ to 800℃ temperature at a rate of 10℃ per minute and kept in isothermal condition for 60 minutes. Simultaneous Thermal Analyzer 6000 (STA 6000, Perkin Elmer, Inc) was used for the first three categories of experiment and SDT Thermal Instrument 2960 was used for coke gasification with carbon dioxide. In both cases alumina crucible pan was used which has melting point of 2000℃. The results of the experiments are analyzed in three broad categories such as: (a) thermal decomposition analysis, (b) energy profile analysis, and (c) kinetic model development to identify apparent kinetic parameter.

It has been noticed from the thermogravimetry analysis of combustion reaction with air of all samples up to 800℃ that lower temperature of DRM reaction promotes deposition of coke and intensifies with elongation of time. In general, decomposition starts above 500℃, at around 700℃ all samples showed a plateau. After analyzing TG curve of combustion reaction with air at different temperatures (700℃, 600℃, 550℃, and

500℃), it has been found that the amount of coke regeneration at around 600℃ and 700℃ is almost same but the only difference is that at higher temperature the reaction occurs faster.

As methane is used in DRM reaction and methane cracking is very essential step of the reaction. Therefore, there is a possibility of deposition of hydrogen containing volatile species together with coke on the catalyst surface. The pyrolysis reaction with nitrogen was done to identify the possible deposition of volatiles with hydrogen. The result of the reaction indicates the possible deposition of hydrogen bearing volatile species together with deposited coke.

More interestingly coke gasification reaction with carbon dioxide has been done to identify the possibility of regeneration using carbon dioxide which is a greenhouse gas. The result of the experiment shows an excellent performance to regenerate the catalyst. This is an added advantage of DRM to reduce these greenhouse gases.

From the heat flow analysis, it can be noticed that several types of components were deposited on the catalyst surface. It also has been identified by the overlap of the peaks that same species of coke is deposited in stratified structure. Therefor after removal of one layer another layer starts to decompose. Low temperature DRM reaction causes deposition of more variety of species on the catalyst surface than the higher temperature DRM reaction.

The kinetic model fitting was done using least square approach to determine the pre-exponential factor, activation energy, and mass fraction of each pseudo component. Generalized Reduced Gradient (GRG) nonlinear algorithm was used in solver tool of Microsoft Excel. The model shows that two types of pseudo components are deposited as coke. At higher temperature of regeneration, both pseudo components can be removed while at lower temperature only one pseudo component can be removed.

The limitation of the experiment was that I could not compare the regenerated catalyst with fresh catalyst to check the performance due to having vary small amount left over after the regeneration reaction. From the experimental observation it can be generalized that development of DRM in the industrial scale would be quite challenging as Ni-based catalyst attract large amount of coke.

References

2020 climate and energy package | Climate Action. (n.d.). Retrieved May 20, 2018, from https://ec.europa.eu/clima/policies/strategies/2020_en

2030 climate and energy framework | Climate Action. (n.d.). Retrieved May 20, 2018, from https://ec.europa.eu/clima/policies/strategies/2030_en

2050 low-carbon economy | Climate Action. (n.d.). Retrieved May 20, 2018, from https://ec.europa.eu/clima/policies/strategies/2050_en

Alenazey, F. S. (2014). Utilizing carbon dioxide as a regenerative agent in methane dry reforming to improve hydrogen production and catalyst activity and longevity. *International Journal of Hydrogen Energy*. https://doi.org/10.1016/j.ijhydene.2014.02.148

Aminu, M. D., Nabavi, S. A., Rochelle, C. A., & Manovic, V. (2017). A review of developments in carbon dioxide storage. *Applied Energy*, *208*(September), 1389–1419. https://doi.org/10.1016/j.apenergy.2017.09.015

Aramouni, N. A. K., Touma, J. G., Tarboush, B. A., Zeaiter, J., & Ahmad, M. N. (2018). Catalyst design for dry reforming of methane: Analysis review. *Renewable and Sustainable Energy Reviews*, *82*(September 2017), 2570–2585. https://doi.org/10.1016/j.rser.2017.09.076

Coelho, A., Costa, L., Marques, M. M., Fonseca, I. M., Lemos, M. A. N. D. A., & Lemos, F. (2012). The effect of ZSM-5 zeolite acidity on the catalytic degradation of high-density polyethylene using simultaneous DSC/TG analysis. *Applied Catalysis A: General*, *413–414*, 183–191. https://doi.org/10.1016/j.apcata.2011.11.010

Dębek, R., Motak, M., Duraczyska, D., Launay, F., Galvez, M. E., Grzybek, T., & Da Costa, P. (2016). Methane dry reforming over hydrotalcite-derived Ni-Mg-Al mixed oxides: The influence of Ni content on catalytic activity, selectivity and stability. *Catalysis Science and Technology*, *6*(17), 6705–6715. https://doi.org/10.1039/c6cy00906a

Dębek, R., Zubek, K., Motak, M., Galvez, M. E., Da Costa, P., & Grzybek, T. (2015). Ni-Al hydrotalcite-like material as the catalyst precursors for the dry reforming of methane at low temperature. *Comptes Rendus Chimie*, *18*(11), 1205–1210. https://doi.org/10.1016/j.crci.2015.04.005

Dsc-tga, S. (n.d.). SDT 2960 Simultaneous DSC-TGA including DTA capabilities.

Gao, Y., Jiang, J., Meng, Y., Yan, F., & Aihemaiti, A. (2018). A review of recent developments in hydrogen production via biogas dry reforming. *Energy Conversion and Management*, *171*(May),

133–155. https://doi.org/10.1016/j.enconman.2018.05.083

Global Greenhouse Gas Emissions Data | Greenhouse Gas (GHG) Emissions | US EPA. (n.d.). Retrieved May 17, 2018, from https://www.epa.gov/ghgemissions/global-greenhouse-gas-emissions-data

Greenhouse gas emission statistics - emission inventories - Statistics Explained. (n.d.). Retrieved May 20, 2018, from http://ec.europa.eu/eurostat/statistics-explained/index.php/Greenhouse_gas_emission_statistics

IPCC. (2014). *Summary for Policymakers*. *Climate Change 2014: Synthesis Report. Contribution of Working Groups I, II and III to the Fifth Assessment Report of the Intergovernmental Panel on Climate Change*. https://doi.org/10.1017/CBO9781107415324

Jang, W. J., Shim, J. O., Kim, H. M., Yoo, S. Y., & Roh, H. S. (2018). A review on dry reforming of methane in aspect of catalytic properties. *Catalysis Today*, (June), 0–1. https://doi.org/10.1016/j.cattod.2018.07.032

Karimi, F., & Toikka, A. (2018). General public reactions to carbon capture and storage: Does culture matter? *International Journal of Greenhouse Gas Control*, *70*(September 2017), 193–201. https://doi.org/10.1016/j.ijggc.2018.01.012

Koytsoumpa, E. I., Bergins, C., & Kakaras, E. (2018). The CO2economy: Review of CO2capture and reuse technologies. *Journal of Supercritical Fluids*, *132*(July 2017), 3–16. https://doi.org/10.1016/j.supflu.2017.07.029

Löfberg, A., Guerrero-Caballero, J., Kane, T., Rubbens, A., & Jalowiecki-Duhamel, L. (2017). Ni/CeO2based catalysts as oxygen vectors for the chemical looping dry reforming of methane for syngas production. *Applied Catalysis B: Environmental*, *212*, 159–174. https://doi.org/10.1016/j.apcatb.2017.04.048

Löfberg, A., Kane, T., Guerrero-Caballero, J., & Jalowiecki-Duhamel, L. (2017). Chemical looping dry reforming of methane: toward shale-gas and biogas valorization. *Chemical Engineering and Processing: Process Intensification*, *122*(April), 523–529. https://doi.org/10.1016/j.cep.2017.05.003

Missen, R. W., Mims, C. A., & Saville, B. A. (n.d.). *Ronald W. Missen Charles A. Mims Bradley A. Saville*.

Potential, B. I. G. (n.d.). SMALL SIZE BIG POTENTIAL.

Takanabe, K., Nagaoka, K., Nariai, K., & Aika, K. I. (2005). Influence of reduction temperature on the catalytic behavior of Co/TiO2catalysts for CH4/CO2reforming and its relation with titania bulk crystal structure. *Journal of Catalysis*, *230*(1), 75–85. https://doi.org/10.1016/j.jcat.2004.11.005

Tapia, J. F. D., Lee, J. Y., Ooi, R. E. H., Foo, D. C. Y., & Tan, R. R. (2018). A review of optimization and decision-making models for the planning of CO2capture, utilization and storage (CCUS) systems. *Sustainable Production and Consumption*, *13*(September), 1–15. https://doi.org/10.1016/j.spc.2017.10.001

Thronicker, D., Lange, I., & Pless, J. (2016). Determining the success of carbon capture and storage projects. *Electricity Journal*, *29*(7), 1–4. https://doi.org/10.1016/j.tej.2016.08.001

Wang, Y., Yao, L., Wang, S., Mao, D., & Hu, C. (2018). Low-temperature catalytic CO2dry reforming of methane on Ni-based catalysts: A review. *Fuel Processing Technology*, *169*(June 2017), 199–206. https://doi.org/10.1016/j.fuproc.2017.10.007

Yao, L., Wang, Y., Shi, J., Xu, H., Shen, W., & Hu, C. (2017). The influence of reduction temperature on the performance of ZrOx/Ni-MnOx/SiO2catalyst for low-temperature CO2reforming of methane. *Catalysis Today*, *281*, 259–267. https://doi.org/10.1016/j.cattod.2016.05.031